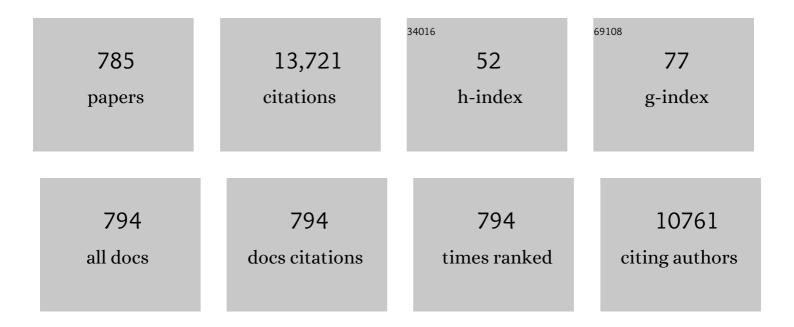
## **Eduardo** Alves

List of Publications by Year in descending order

Source: https://exaly.com/author-pdf/7484251/publications.pdf Version: 2024-02-01



FDUADO ALVES

#	Article	IF	CITATIONS
1	Overview of JET results for optimising ITER operation. Nuclear Fusion, 2022, 62, 042026.	1.6	52
2	Improvement of Mechanical Properties with Non-Equimolar CrNbTaVW High Entropy Alloy. Crystals, 2022, 12, 219.	1.0	4
3	Structural analysis of the ZnO/MgO superlattices on a-polar ZnO substrates grown by MBE. Applied Surface Science, 2022, 587, 152830.	3.1	3
4	Tantalum-Titanium Oxynitride Thin Films Deposited by DC Reactive Magnetron Co-Sputtering: Mechanical, Optical, and Electrical Characterization. Coatings, 2022, 12, 36.	1.2	6
5	Confronting Vegard's rule in Ge <sub>1â^'x </sub> Sn <sub>x</sub> epilayers: from fundamentals to the effect of defects. Journal Physics D: Applied Physics, 2022, 55, 295301.	1.3	2
6	Enhancing the luminescence yield of Cr3+ in <b> <i>β</i> </b> -Ga2O3 by proton irradiation. Applied Physics Letters, 2022, 120, .	1.5	8
7	Dependence of optical properties on composition of silicon carbonitride thin films deposited at low temperature by PECVD. Journal of Non-Crystalline Solids, 2021, 551, 120434.	1.5	7
8	Microwave transient reflection in annealed SnS thin films. Materials Science in Semiconductor Processing, 2021, 121, 105302.	1.9	5
9	The effects of mechanical alloying on the physical and thermal properties of CuCrFeTiV alloy. Materials Science and Engineering B: Solid-State Materials for Advanced Technology, 2021, 263, 114805.	1.7	5
10	Ion beam analysis of Li-Sn alloys for fusion applications. Nuclear Instruments & Methods in Physics Research B, 2021, 486, 55-62.	0.6	0
11	Deposition of Ti-Zr-O-N films by reactive magnetron sputtering of Zr target with Ti ribbons. Surface and Coatings Technology, 2021, 409, 126737.	2.2	3
12	Electrical, optical and photoconductive properties of Sn-doped indium sulfofluoride thin films. Materials Science in Semiconductor Processing, 2021, 121, 105349.	1.9	1
13	Crystal mosaicity determined by a novel layer deconvolution Williamson–Hall method. CrystEngComm, 2021, 23, 2048-2062.	1.3	8
14	Multiple reflection optimization package for X-ray diffraction. CrystEngComm, 2021, 23, 3308-3318.	1.3	6
15	Eu3+ optical activation engineering in Al Ga1-N nanowires for red solid-state nano-emitters. Applied Materials Today, 2021, 22, 100893.	2.3	4
16	Unravelling the secrets of the resistance of GaN to strongly ionising radiation. Communications Physics, 2021, 4, .	2.0	26
17	Simulating the effect of Ar+ energy implantation on the strain propagation in AlGaN. Journal Physics D: Applied Physics, 2021, 54, 245301.	1.3	6
18	Self-powered proton detectors based on GaN core–shell p–n microwires. Applied Physics Letters, 2021, 118, .	1.5	3

#	Article	IF	CITATIONS
19	An insider view of the Portuguese ion beam laboratory. European Physical Journal Plus, 2021, 136, 1.	1.2	15
20	Use of a Timepix position-sensitive detector for Rutherford backscattering spectrometry with channeling. Nuclear Instruments & Methods in Physics Research B, 2021, 499, 61-69.	0.6	2
21	Enhanced red emission from Eu-implanted ZnMgO layers and ZnO/ZnMgO quantum structures. Applied Physics Letters, 2021, 119, .	1.5	4
22	Nonpolar short-period ZnO/MgO superlattices: Radiative excitons analysis. Journal of Luminescence, 2021, 238, 118288.	1.5	4
23	In-situ annealing transmission electron microscopy of plasmonic thin films composed of bimetallic Au–Ag nanoparticles dispersed in a TiO2 matrix. Vacuum, 2021, 193, 110511.	1.6	8
24	Ta2O5/SiO2 Multicomponent Dielectrics for Amorphous Oxide TFTs. Electronic Materials, 2021, 2, 1-16.	0.9	6
25	Fuel retention and erosion-deposition on inner wall cladding tiles in JET-ILW. Physica Scripta, 2021, 96, 124071.	1.2	7
26	Evaluation of tritium retention in plasma facing components during JET tritium operations. Physica Scripta, 2021, 96, 124075.	1.2	14
27	Me-Doped Ti–Me Intermetallic Thin Films Used for Dry Biopotential Electrodes: A Comparative Case Study. Sensors, 2021, 21, 8143.	2.1	5
28	Thin films of Au-Al2O3 for plasmonic sensing. Applied Surface Science, 2020, 500, 144035.	3.1	13
29	Evolution of the mechanical properties of Ti-based intermetallic thin films doped with different metals to be used as biomedical devices. Applied Surface Science, 2020, 505, 144617.	3.1	22
30	Deuterium inventory determination in beryllium and mixed beryllium-carbon layers doped with oxygen. Fusion Engineering and Design, 2020, 150, 111365.	1.0	4
31	Ion beam analysis of fusion plasma-facing materials and components: facilities and research challenges. Nuclear Fusion, 2020, 60, 025001.	1.6	54
32	Estimating the uncertainties of strain and damage analysis by X-ray diffraction in ion implanted MoO3. Nuclear Instruments & Methods in Physics Research B, 2020, 478, 290-296.	0.6	1
33	Lithium dilution in Li-Sn alloys. Nuclear Materials and Energy, 2020, 25, 100783.	0.6	4
34	Ion beam induced current analysis in GaN microwires. EPJ Web of Conferences, 2020, 233, 05001.	0.1	1
35	Nanostructured c-Si surfaces obtained by sequential ion implantation of C+ and Ti+: Tribophysical and structural characterization. Nuclear Instruments & Methods in Physics Research B, 2020, 471, 69-75.	0.6	0

Stopping power of hydrogen in hafnium and the importance of relativistic <mml:math xmlns:mml="http://www.w3.org/1998/Math/MathML"><mml:mrow><mml:mn>4</mml:mn><mml:mi>f</mml:mi><‡roml:mro&></mml:m electrons. Physical Review A, 2020, 101, .

Eduardo Alves

#	Article	IF	CITATIONS
37	Post-mortem analysis of tungsten plasma facing components in tokamaks: Raman microscopy measurements on compact, porous oxide and nitride films and nanoparticles. Nuclear Fusion, 2020, 60, 086004.	1.6	10
38	Oxidation behaviour of neutron irradiated Be pebbles. Nuclear Materials and Energy, 2020, 23, 100748.	0.6	3
39	Fuel inventory and material migration of JET main chamber plasma facing components compared over three operational periods. Physica Scripta, 2020, T171, 014051.	1.2	20
40	Deposition in the tungsten divertor during the 2011–2016 campaigns in JET with ITER-like wall. Physica Scripta, 2020, T171, 014044.	1.2	11
41	Effect of composition and surface characteristics on fuel retention in beryllium-containing co-deposited layers. Physica Scripta, 2020, T171, 014038.	1.2	12
42	Ar <sup>+</sup> ion irradiation of magnetic tunnel junction multilayers: impact on the magnetic and electrical properties. Journal Physics D: Applied Physics, 2020, 53, 455003.	1.3	6
43	W/AlSiTiNx/SiAlTiOyNx/SiAlOx multilayered solar thermal selective absorber coating. Solar Energy, 2020, 207, 192-198.	2.9	18
44	Study of structural and optical properties of MBE grown nonpolar (10-10) ZnO/ZnMgO photonic structures. Optical Materials, 2020, 100, 109709.	1.7	8
45	Nanocomposite Au-ZnO thin films: Influence of gold concentration and thermal annealing on the microstructure and plasmonic response. Surface and Coatings Technology, 2020, 385, 125379.	2.2	8
46	Advanced Monte Carlo Simulations for Ion-Channeling Studies of Complex Defects in Crystals. Springer Series in Materials Science, 2020, , 133-160.	0.4	3
47	Photoelectrochemical Water Splitting: Thermal Annealing Challenges on Hematite Nanowires. Journal of Physical Chemistry C, 2020, 124, 12897-12911.	1.5	24
48	Deuterium retention on the tungsten-coated divertor tiles of JET ITER-like wall in 2015–2016 campaign. Fusion Engineering and Design, 2019, 146, 1979-1982.	1.0	5
49	Micro-Opto-Electro-Mechanical Device Based on Flexible β-Ga <sub>2</sub> O <sub>3</sub> ÂMicro-Lamellas. ECS Journal of Solid State Science and Technology, 2019, 8, Q3235-Q3241.	0.9	3
50	Structural and optical studies of aluminosilicate films doped with (Tb3+, Er3+)/Yb3+ by ion implantation. Nuclear Instruments & Methods in Physics Research B, 2019, 459, 71-75.	0.6	4
51	Metallic filamentary conduction in valence change-based resistive switching devices: the case of TaO <sub>x</sub> thin film with <i>x</i> â^¼ 1. Nanoscale, 2019, 11, 16978-16990.	2.8	16
52	Overview of the JET preparation for deuterium–tritium operation with the ITER like-wall. Nuclear Fusion, 2019, 59, 112021.	1.6	87
53	Direct observation of mono-vacancy and self-interstitial recovery in tungsten. APL Materials, 2019, 7, .	2.2	45
54	New WC-Cu composites for the divertor in fusion reactors. Journal of Nuclear Materials, 2019, 521, 31-37.	1.3	12

4

Eduardo Alves

#	Article	IF	CITATIONS
55	Measuring strain caused by ion implantation in GaN. Materials Science in Semiconductor Processing, 2019, 98, 95-99.	1.9	15
56	Luminescence properties of MOCVD grown Al0.2Ga0.8N layers implanted with Tb. Journal of Luminescence, 2019, 210, 413-424.	1.5	1
57	Deposition of impurity metals during campaigns with the JET ITER-like Wall. Nuclear Materials and Energy, 2019, 19, 218-224.	0.6	23
58	Stability of beryllium coatings deposited on carbon under annealing up to 1073 K. Fusion Engineering and Design, 2019, 146, 303-307.	1.0	4
59	Thin films composed of metal nanoparticles (Au, Ag, Cu) dispersed in AlN: The influence of composition and thermal annealing on the structure and plasmonic response. Thin Solid Films, 2019, 676, 12-25.	0.8	20
60	The effect of increasing Si content in the absorber layers (CrAlSiNx/CrAlSiOyNx) of solar selective absorbers upon their selectivity and thermal stability. Applied Surface Science, 2019, 481, 1096-1102.	3.1	7
61	First mirror test in JET for ITER: Complete overview after three ILW campaigns. Nuclear Materials and Energy, 2019, 19, 59-66.	0.6	24
62	Tritium distributions on W-coated divertor tiles used in the third JET ITER-like wall campaign. Nuclear Materials and Energy, 2019, 18, 258-261.	0.6	10
63	Incorporation of Europium into GaN Nanowires by Ion Implantation. Journal of Physical Chemistry C, 2019, 123, 11874-11887.	1.5	12
64	Engineering strain and conductivity of MoO3 by ion implantation. Acta Materialia, 2019, 169, 15-27.	3.8	19
65	Monte Carlo simulations of ion channeling in crystals containing dislocations and randomly displaced atoms. Journal of Applied Physics, 2019, 126, .	1.1	21
66	Optical and photoconductive properties of indium sulfide fluoride thin films. Thin Solid Films, 2019, 671, 49-52.	0.8	5
67	Influence of Al/Si atomic ratio on optical and electrical properties of magnetron sputtered Al1-xSixOy coatings. Thin Solid Films, 2019, 669, 475-481.	0.8	4
68	Analysis of deposited layers with deuterium and impurity elements on samples from the divertor of JET with ITER-like wall. Journal of Nuclear Materials, 2019, 516, 202-213.	1.3	18
69	Analysis of the outer divertor hot spot activity in the protection video camera recordings at JET. Fusion Engineering and Design, 2019, 139, 115-123.	1.0	3
70	Deposition temperature influence on the wear behaviour of carbon-based coatings deposited on hardened steel. Applied Surface Science, 2019, 475, 762-773.	3.1	9
71	Compositional analysis by RBS, XPS and EDX of ZnO:Al,Bi and ZnO:Ga,Bi thin films deposited by d.c. magnetron sputtering. Vacuum, 2019, 161, 268-275.	1.6	26
72	Improved neutron activation dosimetry for fusion. Fusion Engineering and Design, 2019, 139, 109-114.	1.0	7

#	Article	IF	CITATIONS
73	RBS/C, XRR, and XRD Studies of Damage Buildup in Erâ€Implanted ZnO. Physica Status Solidi (B): Basic Research, 2019, 256, 1800364.	0.7	17
74	CrAlSiN barrier layer to improve the thermal stability of W/CrAlSiNx/CrAlSiOyNx/SiAlOx solar thermal absorber. Solar Energy Materials and Solar Cells, 2019, 191, 235-242.	3.0	17
75	A study of solar thermal absorber stack based on CrAlSiNx/CrAlSiNxOy structure by ion beams. Nuclear Instruments & Methods in Physics Research B, 2019, 450, 195-199.	0.6	5
76	Measurement of proton induced Î <sup>3</sup> -ray emission cross sections on Na from 1.0 to 4.1 MeV. Nuclear Instruments & Methods in Physics Research B, 2019, 441, 108-118.	0.6	8
77	Defect formation and optical activation of Tb implanted AlxGa1â^'xN films using channeled implantation at different temperatures. Surface and Coatings Technology, 2018, 355, 29-39.	2.2	9
78	Helium load on W-O coatings grown by pulsed laser deposition. Surface and Coatings Technology, 2018, 355, 215-221.	2.2	8
79	WC-Cu thermal barriers for fusion applications. Surface and Coatings Technology, 2018, 355, 222-226.	2.2	17
80	Thin films of Ag–Au nanoparticles dispersed in TiO <sub>2</sub> : influence of composition and microstructure on the LSPR and SERS responses. Journal Physics D: Applied Physics, 2018, 51, 205102.	1.3	30
81	Up-conversion emission of aluminosilicate and titania films doped with Er3+/Yb3+ by ion implantation and sol-gel solution doping. Surface and Coatings Technology, 2018, 355, 162-168.	2.2	14
82	Backscattering analysis of short period ZnO/MgO superlattices. Surface and Coatings Technology, 2018, 355, 45-49.	2.2	17
83	Optical investigations of europium ion implanted in nitride-based diode structures. Surface and Coatings Technology, 2018, 355, 40-44.	2.2	9
84	Crystal damage analysis of implanted AlxGa1-xN (0 â‰ <b>å</b> €¯x â‰ <b>å</b> €¯1) by ion beam techniques. Surface and Technology, 2018, 355, 55-60.	Coatings	9
85	Neutron spectroscopy measurements of 14 MeV neutrons at unprecedented energy resolution and implications for deuterium–tritium fusion plasma diagnostics. Measurement Science and Technology, 2018, 29, 045502.	1.4	35
86	A design of selective solar absorber for high temperature applications. Solar Energy, 2018, 172, 177-183.	2.9	38
87	Electrical characterization of molybdenum oxide lamellar crystals irradiated with UV light and proton beams. Surface and Coatings Technology, 2018, 355, 50-54.	2.2	5
88	Helium and deuterium irradiation effects in tungsten-based materials with titanium. Surface and Coatings Technology, 2018, 355, 143-147.	2.2	1
89	Radiation sensors based on GaN microwires. Journal Physics D: Applied Physics, 2018, 51, 175105.	1.3	8
90	Optimization of nanocomposite Au/TiO 2 thin films towards LSPR optical-sensing. Applied Surface Science, 2018, 438, 74-83.	3.1	54

#	Article	IF	CITATIONS
91	Zr-O-N coatings for decorative purposes: Study of the system stability by exploration of the deposition parameter space. Surface and Coatings Technology, 2018, 343, 30-37.	2.2	23
92	In-situ XRD vs ex-situ vacuum annealing of tantalum oxynitride thin films: Assessments on the structural evolution. Applied Surface Science, 2018, 438, 14-19.	3.1	1
93	New WC-Cu thermal barriers for fusion applications: High temperature mechanical behaviour. Journal of Nuclear Materials, 2018, 498, 355-361.	1.3	12
94	Analysis of retained deuterium on Be-based films: Ion implantation vs. in-situ loading. Nuclear Materials and Energy, 2018, 17, 242-247.	0.6	2
95	Deuterium retention and erosion in liquid Sn samples exposed to D2 and Ar plasmas in GyM device. Nuclear Materials and Energy, 2018, 17, 253-258.	0.6	17
96	Multiple optical centers in Eu-implanted AlN nanowires for solid-state lighting applications. Applied Physics Letters, 2018, 113, 201905.	1.5	8
97	CuxCrFeMoTi (x = 0.21, 0.44, 1) high entropy alloys as novel materials for fusion applications. Materials Science and Engineering B: Solid-State Materials for Advanced Technology, 2018, 238-239, 18-25.	1.7	8
98	Thin films composed of Au nanoparticles embedded in AlN: Influence of metal concentration and thermal annealing on the LSPR band. Vacuum, 2018, 157, 414-421.	1.6	24
99	Ion irradiation-induced easy-cone anisotropy in double-MgO free layers for perpendicular magnetic tunnel junctions. Applied Physics Letters, 2018, 112, .	1.5	14
100	In Situ Characterization and Modification of βâ€Ga <sub>2</sub> O <sub>3</sub> Flakes Using an Ion Microâ€Probe. Physica Status Solidi (A) Applications and Materials Science, 2018, 215, 1800190.	0.8	7
101	Eu-Doped AlGaN/GaN Superlattice-Based Diode Structure for Red Lighting: Excitation Mechanisms and Active Sites. ACS Applied Nano Materials, 2018, 1, 3845-3858.	2.4	14
102	Thermal desorption spectrometry of beryllium plasma facing tiles exposed in the JET tokamak. Fusion Engineering and Design, 2018, 133, 135-141.	1.0	19
103	Assessment of erosion, deposition and fuel retention in the JET-ILW divertor from ion beam analysis data. Nuclear Materials and Energy, 2017, 12, 559-563.	0.6	28
104	Deuterium retention in tin (Sn) and lithium–tin (Li–Sn) samples exposed to ISTTOK plasmas. Nuclear Materials and Energy, 2017, 12, 709-713.	0.6	32
105	Behavior of liquid Li-Sn alloy as plasma facing material on ISTTOK. Fusion Engineering and Design, 2017, 117, 208-211.	1.0	18
106	Asymmetric ZnO/ZnMgO double quantum well structures grown on m-plane ZnO substrates by MBE. Journal of Luminescence, 2017, 186, 262-267.	1.5	10
107	Studies of lithium deposition and D retention on tungsten samples exposed to Li-seeded plasmas in PISCES-A. Plasma Physics and Controlled Fusion, 2017, 59, 044006.	0.9	4
108	Efficient temperature sensing using photoluminescence of Er/Yb implanted GaN thin films. Sensors and Actuators B: Chemical, 2017, 248, 769-776.	4.0	39

#	Article	IF	CITATIONS
109	Validity of Vegard's rule for Al1â^'xInxN (0.08  <  x  < aꀉo.28) thin films g Physics D: Applied Physics, 2017, 50, 205107.	grown on (	GaN templates
110	Thermal and chemical stability of the β-W2N nitride phase. Nuclear Materials and Energy, 2017, 12, 462-467.	0.6	20
111	SiGe layer thickness effect on the structural and optical properties of well-organized SiGe/SiO2multilayers. Nanotechnology, 2017, 28, 345701.	1.3	5
112	Optical and structural analysis of solar selective absorbing coatings based on AlSiOx:W cermets. Solar Energy, 2017, 150, 335-344.	2.9	40
113	Helium and deuterium irradiation effects in W-Ta composites produced by pulse plasma compaction. Journal of Nuclear Materials, 2017, 492, 105-112.	1.3	11
114	Study of deuterium retention in Be-W coatings with distinct roughness profiles. Fusion Engineering and Design, 2017, 124, 464-467.	1.0	7
115	Overview of the JET ITER-like wall divertor. Nuclear Materials and Energy, 2017, 12, 499-505.	0.6	46
116	Effects of thermal annealing on the structural and electronic properties of rare earth-implanted MoO <sub>3</sub> nanoplates. CrystEngComm, 2017, 19, 2339-2348.	1.3	6
117	Fuel inventory and deposition in castellated structures in JET-ILW. Nuclear Fusion, 2017, 57, 066027.	1.6	25
118	Characterization of magnetron sputtered sub-stoichiometric CrAlSiN x and CrAlSiO y N x coatings. Surface and Coatings Technology, 2017, 328, 134-141.	2.2	18
119	Investigation and plasma cleaning of first mirrors coated with relevant ITER contaminants: beryllium and tungsten. Nuclear Fusion, 2017, 57, 086019.	1.6	17
120	Overview of the JET results in support to ITER. Nuclear Fusion, 2017, 57, 102001.	1.6	150
121	Overview of fuel inventory in JET with the ITER-like wall. Nuclear Fusion, 2017, 57, 086045.	1.6	47
122	Impurity re-distribution in the corner regions of the JET divertor. Physica Scripta, 2017, T170, 014060.	1.2	6
123	Experience on divertor fuel retention after two ITER-Like Wall campaigns. Physica Scripta, 2017, T170, 014063.	1.2	26
124	Doping β-Ga <sub>2</sub> O <sub>3</sub> with europium: influence of the implantation and annealing temperature. Journal Physics D: Applied Physics, 2017, 50, 325101.	1.3	26
125	Implantation damage formation in a-, c- and m-plane GaN. Acta Materialia, 2017, 123, 177-187.	3.8	73
126	Formation of metastable phases in Zr-ion-irradiated Al2O3 upon thermal annealing. Journal of Electron Microscopy, 2017, 66, 388-396.	0.9	0

#	Article	IF	CITATIONS
127	Assessing material properties for fusion applications by ion beams. Nuclear Instruments & Methods in Physics Research B, 2017, 409, 255-258.	0.6	2
128	Time-resolved deposition in the remote region of the JET-ILW divertor: measurements and modelling. Physica Scripta, 2017, T170, 014059.	1.2	6
129	Plasma–wall interaction studies within the EUROfusion consortium: progress on plasma-facing components development and qualification. Nuclear Fusion, 2017, 57, 116041.	1.6	75
130	Corrosion Behavior of Titanium Oxynitrided by Diffusion and Magnetron Sputtering Methods in Physiological Solution. Materials Performance and Characterization, 2017, 6, 594-606.	0.2	0
131	Nanoscale triboactivity of functionalized c-Si surfaces by Fe <sup>+</sup> ion implantation. Journal of Physics Condensed Matter, 2016, 28, 134003.	0.7	1
132	Ag:TiN oated Polyurethane for Dry Biopotential Electrodes: From Polymer Plasma Interface Activation to the First EEG Measurements. Plasma Processes and Polymers, 2016, 13, 341-354.	1.6	27
133	Impact of implantation geometry and fluence on structural properties of AlxGa1-xN implanted with thulium. Journal of Applied Physics, 2016, 120, .	1.1	10
134	High Orbital Angular Momentum Harmonic Generation. Physical Review Letters, 2016, 117, 265001.	2.9	66
135	Utilization of native oxygen in Eu(RE)-doped GaN for enabling device compatibility in optoelectronic applications. Scientific Reports, 2016, 6, 18808.	1.6	29
136	Identifying the influence of the intrinsic defects in Gd-doped ZnO thin-films. Journal of Applied Physics, 2016, 119, .	1.1	52
137	Spectroscopic analysis of the NIR emission in Tm implanted AlxGa1-xN layers. Journal of Applied Physics, 2016, 120, 081701.	1.1	9
138	Correction to "Spectroscopic Analysis of Eu <sup>3+</sup> Implanted and Annealed GaN Layers and Nanowires― Journal of Physical Chemistry C, 2016, 120, 6907-6908.	1.5	5
139	Composition measurement of epitaxial Sc <sub><i>x</i></sub> Ga <sub>1â^'<i>x</i></sub> N films. Semiconductor Science and Technology, 2016, 31, 064002.	1.0	3
140	Quantitative x-ray diffraction analysis of bimodal damage distributions in Tm implanted Al <sub>0.15</sub> Ga <sub>0.85</sub> N. Journal Physics D: Applied Physics, 2016, 49, 135308.	1.3	19
141	Electrical insulation properties of RF-sputtered LiPON layers towards electrochemical stability of lithium batteries. Journal Physics D: Applied Physics, 2016, 49, 485301.	1.3	7
142	Determination of 9Be(p,p0)9Be, 9Be(p,d0)8Be and 9Be(p,α0)6Li cross sections at 150° in the energy range 0.5–2.35 MeV. Nuclear Instruments & Methods in Physics Research B, 2016, 371, 50-53.	0.6	9
143	Anisotropy of electrical conductivity in dc due to intrinsic defect formation in α-Al2O3 single crystal implanted with Mg ions. Nuclear Instruments & Methods in Physics Research B, 2016, 379, 91-94.	0.6	1
144	Analysis of the Tb3+ recombination in ion implanted Al Ga1â^'N (Oâ‰æâ‰⊉) layers. Journal of Luminescence, 2016, 178, 249-258.	1.5	7

#	Article	IF	CITATIONS
145	The role and application of ion beam analysis for studies of plasma-facing components in controlled fusion devices. Nuclear Instruments & Methods in Physics Research B, 2016, 371, 4-11.	0.6	18
146	Study of nuclear reactions producing <sup>36</sup> Cl by micro-AMS. Journal of Physics: Conference Series, 2016, 665, 012077.	0.3	1
147	Magnetoelectric effect probe through ppm Fe doping in BaTiO 3. Journal of Alloys and Compounds, 2016, 661, 495-500.	2.8	6
148	Functional behaviour of TiO <sub>2</sub> films doped with noble metals. Surface Engineering, 2016, 32, 554-561.	1.1	14
149	Deposition in the inner and outer corners of the JET divertor with carbon wall and metallic ITER-like wall. Physica Scripta, 2016, T167, 014052.	1.2	14
150	Study of damage formation and annealing of implanted III-nitride semiconductors for optoelectronic devices. Nuclear Instruments & Methods in Physics Research B, 2016, 379, 251-254.	0.6	17
151	Electrochemical characterization of nanostructured Ag:TiN thin films produced by glancing angle deposition on polyurethane substrates for bio-electrode applications. Journal of Electroanalytical Chemistry, 2016, 768, 110-120.	1.9	12
152	Long-term fuel retention in JET ITER-like wall. Physica Scripta, 2016, T167, 014075.	1.2	52
153	Mechanisms of Implantation Damage Formation in Al <sub><i>x</i></sub> Ga <sub>1–<i>x</i></sub> N Compounds. Journal of Physical Chemistry C, 2016, 120, 7277-7283.	1.5	33
154	Quantum well intermixing and radiation effects in InGaN/GaN multi quantum wells. , 2016, , .		1
155	Raman microscopy investigation of beryllium materials. Physica Scripta, 2016, T167, 014027.	1.2	14
156	Study of In distribution on GaInSb:Al crystals by ion beam techniques. Nuclear Instruments & Methods in Physics Research B, 2016, 371, 278-282.	0.6	6
157	Effect of AlN content on the lattice site location of terbium ions in Al <sub><i>x</i></sub> Ga <sub>1â^'<i>x</i></sub> N compounds. Semiconductor Science and Technology, 2016, 31, 035026.	1.0	12
158	Quantitative Chemical Mapping of InGaN Quantum Wells from Calibrated High-Angle Annular Dark Field Micrographs. Microscopy and Microanalysis, 2015, 21, 994-1005.	0.2	3
159	Growth of mixed materials in the Be/W/O system in fusion devices. Microscopy and Microanalysis, 2015, 21, 94-95.	0.2	0
160	W-Ta Composites Consolidated by Spark Plasma Sintering. Microscopy and Microanalysis, 2015, 21, 27-28.	0.2	0
161	Luminescence studies on green emitting InGaN/GaN MQWs implanted with nitrogen. Scientific Reports, 2015, 5, 9703.	1.6	19
162	Photoluminescence studies of a perceived white light emission from a monolithic InGaN/GaN quantum well structure. Scientific Reports, 2015, 5, 13739.	1.6	19

#	Article	IF	CITATIONS
163	Analysis of rotating collectors from the private region of JET with carbon wall and metallic ITER-like wall. Journal of Nuclear Materials, 2015, 463, 818-821.	1.3	9
164	Raman study of insulating and conductive ZnO:(Al, Mn) thin films. Physica Status Solidi (A) Applications and Materials Science, 2015, 212, 2345-2354.	0.8	16
165	Analysis of the stability of InGaN/GaN multiquantum wells against ion beam intermixing. Nanotechnology, 2015, 26, 425703.	1.3	6
166	The effect of metalâ€rich growth conditions on the microstructure of Sc <i><sub>x</sub></i> Ga <sub>1â^²<i>x</i></sub> N films grown using molecular beam epitaxy. Physica Status Solidi (A) Applications and Materials Science, 2015, 212, 2837-2842.	0.8	14
167	Tribological characterization of TiO 2 /Au decorative thin films obtained by PVD magnetron sputtering technology. Wear, 2015, 330-331, 419-428.	1.5	13
168	Fuel retention in JET ITER-Like Wall from post-mortem analysis. Journal of Nuclear Materials, 2015, 463, 961-965.	1.3	50
169	Multifunctional Ti–Me (Me=Al, Cu) thin film systems for biomedical sensing devices. Vacuum, 2015, 122, 353-359.	1.6	20
170	Structural characterization of dual ion implantation in silicon. Nuclear Instruments & Methods in Physics Research B, 2015, 365, 39-43.	0.6	4
171	Laser-induced diffusion decomposition in Fe–V thin-film alloys. Applied Surface Science, 2015, 336, 380-384.	3.1	2
172	Solar selective absorbers based on Al2O3:W cermets and AlSiN/AlSiON layers. Solar Energy Materials and Solar Cells, 2015, 137, 93-100.	3.0	68
173	Determination of the 9Be(3He,pi)11B (i=0,1,2,3) cross section at 135° in the energy range 1–2.5MeV. Nuclear Instruments & Methods in Physics Research B, 2015, 346, 21-25.	0.6	24
174	Electrochemical and structural characterization of nanocomposite Agy:TiNx thin films for dry bioelectrodes: the effect of the N/Ti ratio and Ag content. Electrochimica Acta, 2015, 153, 602-611.	2.6	9
175	Study of the electrical behavior of nanostructured Ti–Ag thin films, prepared by Glancing Angle Deposition. Materials Letters, 2015, 157, 188-192.	1.3	13
176	Corundum-to-spinel structural phase transformation in alumina. Nuclear Instruments & Methods in Physics Research B, 2015, 358, 136-141.	0.6	12
177	Biological behaviour of thin films consisting of Au nanoparticles dispersed in a TiO2 dielectric matrix. Vacuum, 2015, 122, 360-368.	1.6	20
178	Spectroscopic Analysis of Eu <sup>3+</sup> Implanted and Annealed GaN Layers and Nanowires. Journal of Physical Chemistry C, 2015, 119, 17954-17964.	1.5	13
179	Ag y :TiN x thin films for dry biopotential electrodes: the effect of composition and structural changes on the electrical and mechanical behaviours. Applied Physics A: Materials Science and Processing, 2015, 119, 169-178.	1.1	2
180	Composition, structure and morphology of Al <sub>1â^'<i>x</i></sub> In <sub><i>x</i></sub> N thin films grown on Al <sub>1â^'<i>y</i></sub> Ga <sub><i>y</i></sub> N templates with different GaN contents. Journal Physics D: Applied Physics, 2015, 48, 015103.	1.3	7

#	Article	IF	CITATIONS
181	Peculiar Magnetoelectric Coupling in BaTiO <sub>3</sub> :Fe <sub>113Âppm</sub> Nanoscopic Segregations. ACS Applied Materials & Interfaces, 2015, 7, 24741-24747.	4.0	9
182	Structure dependent resistivity and dielectric characteristics of tantalum oxynitride thin films produced by magnetron sputtering. Applied Surface Science, 2015, 354, 298-305.	3.1	14
183	Retention behaviour of deuterium and helium in beryllium under single D+ and dual He+/D+ exposure. Fusion Engineering and Design, 2015, 98-99, 1362-1366.	1.0	4
184	Composition and structure variation for magnetron sputtered tantalum oxynitride thin films, as function of deposition parameters. Applied Surface Science, 2015, 358, 508-517.	3.1	7
185	Clobal erosion and deposition patterns in JET with the ITER-like wall. Journal of Nuclear Materials, 2015, 463, 157-161.	1.3	48
186	Consolidation of W–Ta composites: Hot isostatic pressing and spark and pulse plasma sintering. Fusion Engineering and Design, 2015, 98-99, 1950-1955.	1.0	31
187	Optical properties of zirconium oxynitride films: The effect of composition, electronic and crystalline structures. Applied Surface Science, 2015, 358, 660-669.	3.1	19
188	Optical performance of thin films produced by the pulsed laser deposition of SiAlON and Er targets. Applied Surface Science, 2015, 336, 274-277.	3.1	6
189	Evolution of the functional properties of titanium–silver thin films for biomedical applications: Influence of in-vacuum annealing. Surface and Coatings Technology, 2015, 261, 262-271.	2.2	19
190	An overview of the comprehensive First Mirror Test in JET with ITER-like wall. Physica Scripta, 2014, T159, 014011.	1.2	59
191	High In-content InGaN layers synthesized by plasma-assisted molecular-beam epitaxy: Growth conditions, strain relaxation, and In incorporation kinetics. Journal of Applied Physics, 2014, 116, .	1.1	36
192	Intense luminescence emission from rare-earth-doped MoO3nanoplates and lamellar crystals for optoelectronic applications. Journal Physics D: Applied Physics, 2014, 47, 355105.	1.3	28
193	GaN:Pr <sup>3+</sup> nanostructures for red solid state light emission. RSC Advances, 2014, 4, 62869-62877.	1.7	5
194	Material migration patterns and overview of first surface analysis of the JET ITER-like wall. Physica Scripta, 2014, T159, 014010.	1.2	75
195	Doping of Ga <sub>2</sub> O <sub>3</sub> bulk crystals and NWs by ion implantation. Proceedings of SPIE, 2014, , .	0.8	12
196	First results and surface analysis strategy for plasma-facing components after JET operation with the ITER-like wall. Physica Scripta, 2014, T159, 014016.	1.2	30
197	Laser-assisted cleaning of beryllium-containing mirror samples from JET and PISCES-B. Fusion Engineering and Design, 2014, 89, 122-130.	1.0	23
198	Stopping power of 1H and 4He in lithium niobate. Nuclear Instruments & Methods in Physics Research B, 2014, 332, 330-333.	0.6	3

#	Article	IF	CITATIONS
199	Study of the relationship between crystal structure and luminescence in rare-earth-implanted Ga2O3 nanowires during annealing treatments. Journal of Materials Science, 2014, 49, 1279-1285.	1.7	29
200	Measurement of proton induced $\hat{l}^3$ -ray emission cross sections on Al from 2.5 to 4.1MeV. Nuclear Instruments & Methods in Physics Research B, 2014, 332, 355-358.	0.6	16
201	Optimisation of surface treatments of TiO2:Nb transparent conductive coatings by a post-hot-wire annealing in a reducing H2 atmosphere. Thin Solid Films, 2014, 550, 404-412.	0.8	20
202	Electrochemical behaviour of nanocomposite Agx:TiN thin films for dry biopotential electrodes. Electrochimica Acta, 2014, 125, 48-57.	2.6	30
203	Ion beam induced epitaxial crystallization of α-Al2O3 at room temperature. Nuclear Instruments & Methods in Physics Research B, 2014, 321, 8-13.	0.6	15
204	Structural and optical properties of Ga auto-incorporated InAlN epilayers. Journal of Crystal Growth, 2014, 408, 97-101.	0.7	19
205	Europiumâ€doped GaN(Mg): beyond the limits of the lightâ€emitting diode. Physica Status Solidi C: Current Topics in Solid State Physics, 2014, 11, 662-665.	0.8	17
206	Thermal Properties of Holmium-Implanted Gold Films. Journal of Low Temperature Physics, 2014, 176, 979-985.	0.6	1
207	Determination of Ga auto-incorporation in nominal InAlN epilayers grown by MOCVD. Journal of Materials Chemistry C, 2014, 2, 5787.	2.7	21
208	Surface analysis of tiles and samples exposed to the first JET campaigns with the ITER-like wall. Physica Scripta, 2014, T159, 014012.	1.2	35
209	Stopping power of C, O and Cl in tantalum oxide. Nuclear Instruments & Methods in Physics Research B, 2014, 332, 152-155.	0.6	5
210	Performance of resistive-charge position sensitive detectors for RBS/Channeling applications. Nuclear Instruments and Methods in Physics Research, Section A: Accelerators, Spectrometers, Detectors and Associated Equipment, 2014, 760, 98-106.	0.7	5
211	IBA study of SiGe/SiO2 nanostructured multilayers. Nuclear Instruments & Methods in Physics Research B, 2014, 331, 89-92.	0.6	3
212	Sequential multiple-step europium ion implantation and annealing of GaN. Physica Status Solidi C: Current Topics in Solid State Physics, 2014, 11, 253-257.	0.8	9
213	Composition and luminescence studies of InGaN epilayers grown at different hydrogen flow rates. Semiconductor Science and Technology, 2013, 28, 065011.	1.0	13
214	On the formation of an interface amorphous layer in nanostructured ferroelectric Ba0.8Sr0.2TiO3 thin films integrated on Pt–Si and its effect on the electrical properties. Applied Surface Science, 2013, 278, 136-141.	3.1	11
215	Influence of RF-sputtering power on formation of vertically stacked Si <sub>1â~<i>x</i></sub> Ge <sub><i>x</i></sub> nanocrystals between ultra-thin amorphous Al <sub>2</sub> O <sub>3</sub> layers: structural and photoluminescence properties. Journal Physics D: Applied Physics. 2013, 46, 385301.	1.3	1
216	TiAgx thin films for lower limb prosthesis pressure sensors: Effect of composition and structural changes on the electrical and thermal response of the films. Applied Surface Science, 2013, 285, 10-18.	3.1	34

#	Article	IF	CITATIONS
217	Nanocomposite Ag:TiN thin films for dry biopotential electrodes. Applied Surface Science, 2013, 285, 40-48.	3.1	38
218	Status of the MARE Experiment. IEEE Transactions on Applied Superconductivity, 2013, 23, 2101204-2101204.	1.1	3
219	Influence of stoichiometry and structure on the optical properties of AlN <sub>x</sub> O <sub>y</sub> films. Journal Physics D: Applied Physics, 2013, 46, 015305.	1.3	24
220	Microstructure and nanomechanical properties of Fe+ implanted silicon. Applied Surface Science, 2013, 284, 533-539.	3.1	7
221	Structural and luminescence properties of Eu and Er implanted Bi2O3 nanowires for optoelectronic applications. Journal of Materials Chemistry C, 2013, 1, 7920.	2.7	38
222	p-Type <formula formulatype="inline"><tex Notation="TeX"&gt;\${hbox{Cu}}_{x}{hbox{O}}\$ </tex </formula> Thin-Film Transistors Produced by Thermal Oxidation. Journal of Display Technology, 2013, 9, 735-740.	1.3	34
223	CdTe nano-structures for photovoltaic devices. Nuclear Instruments & Methods in Physics Research B, 2013, 306, 218-221.	0.6	2
224	The influence of photon excitation and proton irradiation on the luminescence properties of yttria stabilized zirconia doped with praseodymium ions. Nuclear Instruments & Methods in Physics Research B, 2013, 306, 207-211.	0.6	2
225	Enhanced red emission from praseodymium-doped GaN nanowires by defect engineering. Acta Materialia, 2013, 61, 3278-3284.	3.8	22
226	Editorial – 13th ICNMTA 2012. Nuclear Instruments & Methods in Physics Research B, 2013, 306, 1-2.	0.6	0
227	Formation of oriented nickel aggregates in rutile single crystals by Ni implantation. Journal of Magnetism and Magnetic Materials, 2013, 340, 102-108.	1.0	7
228	Properties of tantalum oxynitride thin films produced by magnetron sputtering: The influence of processing parameters. Vacuum, 2013, 98, 63-69.	1.6	33
229	Lattice site location and luminescence studies of AlxGa1â^'xN alloys doped with thulium ions. Nuclear Instruments & Methods in Physics Research B, 2013, 307, 495-498.	0.6	6
230	Blistering of W–Ta composites at different irradiation energies. Journal of Nuclear Materials, 2013, 438, S1032-S1035.	1.3	20
231	Effects of helium and deuterium irradiation on SPS sintered W–Ta composites at different temperatures. Journal of Nuclear Materials, 2013, 442, S251-S255.	1.3	17
232	Measurement and evaluation of the 13C(p,p)13C cross section in the energy range 0.8–2.4MeV. Nuclear Instruments & Methods in Physics Research B, 2013, 316, 81-87.	0.6	5
233	Synergistic helium and deuterium blistering in tungsten–tantalum composites. Journal of Nuclear Materials, 2013, 442, 69-74.	1.3	21
234	Development of tantalum oxynitride thin films produced by PVD: Study of structural stability. Applied Surface Science, 2013, 285, 19-26.	3.1	13

#	Article	IF	CITATIONS
235	Formation and delamination of beryllium carbide films. Journal of Nuclear Materials, 2013, 442, S320-S324.	1.3	11
236	A comparative study of photo-, cathodo- and ionoluminescence of GaN nanowires implanted with rare earth ions. Nuclear Instruments & Methods in Physics Research B, 2013, 306, 201-206.	0.6	8
237	Local deposition of 13C tracer in the JET MKII-HD divertor. Journal of Nuclear Materials, 2013, 438, S762-S765.	1.3	1
238	Saturation of hydrogen retention in gallium samples exposed to tokamak ISTTOK plasmas. Journal of Nuclear Materials, 2013, 438, S992-S995.	1.3	2
239	Nanostructures and thin films of transparent conductive oxides studied by perturbed angular correlations. Physica Status Solidi (B): Basic Research, 2013, 250, 801-808.	0.7	4
240	Microprobe analysis, iono- and photo-luminescence of Mn2+ activated ZnGa2O4 fibres. Nuclear Instruments & Methods in Physics Research B, 2013, 306, 195-200.	0.6	12
241	Extended-Gate ISFETs Based on Sputtered Amorphous Oxides. Journal of Display Technology, 2013, 9, 729-734.	1.3	16
242	Towards the understanding of the intentionally induced yellow luminescence in GaN nanowires. Physica Status Solidi C: Current Topics in Solid State Physics, 2013, 10, 667-672.	0.8	8
243	Influence of composition, bonding characteristics and microstructure on the electrochemical and optical stability of AlOxNy thin films. Electrochimica Acta, 2013, 106, 23-34.	2.6	11
244	Comparison of low- and room-temperature damage formation in Ar ion implanted GaN and ZnO. Nuclear Instruments & Methods in Physics Research B, 2013, 307, 394-398.	0.6	34
245	Temperature-dependent hysteresis of the emission spectrum of Eu-implanted, Mg-doped HVPE GaN. AIP Conference Proceedings, 2013, , .	0.3	5
246	Thermal properties of holmium-implanted gold films for a neutrino mass experiment with cryogenic microcalorimeters. Review of Scientific Instruments, 2013, 84, 083905.	0.6	6
247	On the origin of strain relaxation in epitaxial CdZnO layers. , 2013, , .		0
248	Spectroscopy of radiation defects in rutile TiO <sub>2</sub> . Physica Status Solidi (B): Basic Research, 2013, 250, 843-849.	0.7	2
249	The defect structure of sapphire produced by implantation of Zr and Zr plus O: threshold fluence for amorphization and optical properties. Physica Status Solidi C: Current Topics in Solid State Physics, 2013, 10, 202-207.	0.8	2
250	Disorder induced violet/blue luminescence in rfâ€deposited ZnO films. Physica Status Solidi C: Current Topics in Solid State Physics, 2013, 10, 662-666.	0.8	13
251	Investigation of generation of defects due to metallization on CdZnTe detectors. Journal Physics D: Applied Physics, 2012, 45, 175102.	1.3	14
252	Structural and Electrical Properties of Nanostructured Ba <sub>0.8</sub> Sr <sub>0.2</sub> TiO <sub>3</sub> Films Deposited by Pulsed Laser Deposition. Journal of Nano Research, 2012, 18-19, 299-306.	0.8	0

#	Article	IF	CITATIONS
253	TiO <sub>2</sub> coatings with Au nanoparticles analysed by photothermal IR radiometry. Journal Physics D: Applied Physics, 2012, 45, 105301.	1.3	17
254	Tuning the properties of Ge-quantum dots superlattices in amorphous silica matrix through deposition conditions. Journal of Applied Physics, 2012, 111, 074316.	1.1	4
255	Ion beams as a tool for the characterization of near-pseudomorphic CdZnO epilayers. , 2012, , .		1
256	Enhanced dynamic annealing and optical activation of Eu implanted a-plane GaN. Europhysics Letters, 2012, 97, 68004.	0.7	15
257	Structural and magnetic properties of thin films of BaFeO3-δ deposited by pulsed injection metal-organic chemical vapor deposition. Journal of Applied Physics, 2012, 111, .	1.1	9
258	Electroless deposition of Au, Pt, or Ru metallic layers on CdZnTe. Thin Solid Films, 2012, 525, 56-63.	0.8	16
259	Carbon Deposition on Beryllium Substrates and Subsequent Delamination. Materials Science Forum, 2012, 730-732, 179-184.	0.3	Ο
260	Influence of annealing conditions on the formation of regular lattices of voids and Ge quantum dots in an amorphous alumina matrix. Nanotechnology, 2012, 23, 405605.	1.3	8
261	Single phase a-plane MgZnO epilayers for UV optoelectronics: substitutional behaviour of Mg at large contents. CrystEngComm, 2012, 14, 1637-1640.	1.3	29
262	Electrical properties of AlNxOy thin films prepared by reactive magnetron sputtering. Thin Solid Films, 2012, 520, 6709-6717.	0.8	24
263	Optical properties of LFZ grown β-Ga2O3:Eu3+ fibres. Applied Surface Science, 2012, 258, 9157-9161.	3.1	28
264	The influence of annealing treatments on the properties of Ag:TiO2 nanocomposite films prepared by magnetron sputtering. Applied Surface Science, 2012, 258, 4028-4034.	3.1	49
265	Deposition of nanometric double layers Ru/Au, Ru/Pd, and Pd/Au onto CdZnTe by the electroless method. Journal of Crystal Growth, 2012, 358, 89-93.	0.7	9
266	TiNx coated polycarbonate for bio-electrode applications. Corrosion Science, 2012, 56, 49-57.	3.0	37
267	Doped gallium oxide nanowires for photonics. Proceedings of SPIE, 2012, , .	0.8	10
268	Characterization of TiAlSiN/TiAlSiON/SiO2 optical stack designed by modelling calculations for solar selective applications. Solar Energy Materials and Solar Cells, 2012, 105, 202-207.	3.0	70
269	Damage formation and recovery in Fe implanted 6H–SiC. Nuclear Instruments & Methods in Physics Research B, 2012, 286, 89-92.	0.6	4
270	Surface morphology, thermal and electrical conductivity of α-Al2O3 single crystals implanted with Au and Ag ions. Nuclear Instruments & Methods in Physics Research B, 2012, 286, 184-189.	0.6	4

#	Article	IF	CITATIONS
271	Cd ion implantation in AlN. Nuclear Instruments & Methods in Physics Research B, 2012, 289, 43-46.	0.6	6
272	High pressure annealing of Europium implanted GaN. Proceedings of SPIE, 2012, , .	0.8	23
273	Structural and electrical studies of ultrathin layers with Si0.7Ge0.3 nanocrystals confined in a SiGe/SiO2 superlattice. Journal of Applied Physics, 2012, 111, 104323.	1.1	10
274	Electronic structure of ytterbium-implanted GaN at ambient and high pressure: experimental and crystal field studies. Journal of Physics Condensed Matter, 2012, 24, 095803.	0.7	1
275	The electronic transport mechanism in indium molybdenum oxide thin films RF sputtered at room temperature. Europhysics Letters, 2012, 97, 36002.	0.7	9
276	Optical doping of Al[sub x]Ga[sub 1â^'x]N compounds by ion implantation of Tm ions. AlP Conference Proceedings, 2012, , .	0.3	5
277	Unintentional incorporation of H and related structural and freeâ€electron properties of <i>c</i> ―and <i>a</i> â€plane InN. Physica Status Solidi (A) Applications and Materials Science, 2012, 209, 91-94.	0.8	4
278	Ion implantation of Cd and Ag into AlN and GaN. Physica Status Solidi C: Current Topics in Solid State Physics, 2012, 9, 1060-1064.	0.8	9
279	Rare earth co-doping nitride layers for visible light. Materials Chemistry and Physics, 2012, 134, 716-720.	2.0	16
280	Structural and optical studies of Au doped titanium oxide films. Nuclear Instruments & Methods in Physics Research B, 2012, 272, 61-65.	0.6	16
281	Stopping power of He, C and O in TiO2. Nuclear Instruments & Methods in Physics Research B, 2012, 273, 22-25.	0.6	8
282	Stopping power of He, C and O in GaN. Nuclear Instruments & Methods in Physics Research B, 2012, 273, 26-29.	0.6	3
283	Stopping power of C in Si. Nuclear Instruments & Methods in Physics Research B, 2012, 273, 30-32.	0.6	5
284	High precision determination of the InN content of Al1â^'xInxN thin films by Rutherford backscattering spectrometry. Nuclear Instruments & Methods in Physics Research B, 2012, 273, 105-108.	0.6	8
285	Incorporation of N in TiO2 films grown by DC-reactive magnetron sputtering. Nuclear Instruments & Methods in Physics Research B, 2012, 273, 109-112.	0.6	13
286	AIN content influence on the properties of AlxGa1â^'xN doped with Pr ions. Nuclear Instruments & Methods in Physics Research B, 2012, 273, 149-152.	0.6	4
287	Characterization of nanostructured HfO2 films using RBS and PAC. Nuclear Instruments & Methods in Physics Research B, 2012, 273, 195-198.	0.6	1
288	Analysis of multifunctional titanium oxycarbide films as a function of oxygen addition. Surface and Coatings Technology, 2012, 206, 2525-2534.	2.2	27

#	Article	IF	CITATIONS
289	Tuning of the surface plasmon resonance in TiO2/Au thin films grown by magnetron sputtering: The effect of thermal annealing. Journal of Applied Physics, 2011, 109, .	1.1	74
290	Electroless plating of Au, Pt, or Ru thin film layer on CdZnTe. , 2011, , .		1
291	Cathodoluminescence of rare earth implanted Ga2O3and GeO2nanostructures. Nanotechnology, 2011, 22, 285706.	1.3	39
292	Radiation damage formation and annealing in GaN and ZnO. Proceedings of SPIE, 2011, , .	0.8	54
293	Resonant Raman scattering in ZnO:Mn and ZnO:Mn:Al thin films grown by RF sputtering. Journal of Physics Condensed Matter, 2011, 23, 334205.	0.7	26
294	Comparative study of fusion relevant properties of Be12V and Be12Ti. Fusion Engineering and Design, 2011, 86, 2454-2457.	1.0	9
295	Microstructural characterization of the ODS Eurofer 97 EU-batch. Fusion Engineering and Design, 2011, 86, 2386-2389.	1.0	12
296	Tritium permeation, retention and release properties of beryllium pebbles. Fusion Engineering and Design, 2011, 86, 2338-2342.	1.0	9
297	Hydrogen retention in gallium samples exposed to ISTTOK plasmas. Fusion Engineering and Design, 2011, 86, 2458-2461.	1.0	4
298	Surface composition and morphology changes of JET tiles under plasma interactions. Fusion Engineering and Design, 2011, 86, 2557-2560.	1.0	6
299	Deposition of 13C tracer in the JET MkII-HD divertor. Physica Scripta, 2011, T145, 014004.	1.2	15
300	Optical properties of AlN x O y thin films deposited by DC magnetron sputtering. , 2011, , .		3
301	Mass spectrometry improvement on an high current ion implanter. Nuclear Instruments & Methods in Physics Research B, 2011, 269, 3222-3225.	0.6	0
302	Materials research under ITER-like divertor conditions at FOM Rijnhuizen. Journal of Nuclear Materials, 2011, 417, 457-462.	1.3	1
303	Tungsten–microdiamond composites for plasma facing components. Journal of Nuclear Materials, 2011, 416, 45-48.	1.3	6
304	Effect of Eu-implantation and annealing on the GaN quantum dots excitonic recombination. Nanoscale Research Letters, 2011, 6, 378.	3.1	6
305	Colossal dielectric constant of poly- and single-crystalline CaCu3Ti4O12 fibres grown by the laser floating zone technique. Acta Materialia, 2011, 59, 102-111.	3.8	27
306	Low-temperature fabrication of layered self-organized Ge clusters by RF-sputtering. Nanoscale Research Letters, 2011, 6, 341.	3.1	18

#	Article	IF	CITATIONS
307	Free electron properties and hydrogen in InN grown by MOVPE. Physica Status Solidi (A) Applications and Materials Science, 2011, 208, 1179-1182.	0.8	9
308	Comparison of radiation detector performance for different metal contacts on CdZnTe deposited by electroless deposition method. Crystal Research and Technology, 2011, 46, 1131-1136.	0.6	24
309	Ageing effects on the wettability behavior of laser textured silicon. Applied Surface Science, 2011, 257, 2604-2609.	3.1	16
310	Preparation and characterization of CrNxOy thin films: The effect of composition and structural features on the electrical behavior. Applied Surface Science, 2011, 257, 9120-9124.	3.1	19
311	The photoluminescence/excitation (PL/E) spectroscopy of Eu-implanted GaN. Optical Materials, 2011, 33, 1063-1065.	1.7	27
312	Rapid thermal annealing of rare earth implanted ZnO epitaxial layers. Optical Materials, 2011, 33, 1139-1142.	1.7	33
313	The role of the annealing temperature on the optical and structural properties of Eu doped GaN/AlN QD. Optical Materials, 2011, 33, 1045-1049.	1.7	3
314	Influence of the deposition parameters on the growth of SiGe nanocrystals embedded in Al2O3 matrix. Microelectronic Engineering, 2011, 88, 509-513.	1.1	8
315	Structural and optical properties of Er implanted AlN thin films: Green and infrared photoluminescence at room temperature. Optical Materials, 2011, 33, 1055-1058.	1.7	11
316	Mechanisms of damage formation in Eu-implanted GaN probed by X-ray diffraction. Europhysics Letters, 2011, 96, 46002.	0.7	39
317	The high sensitivity of InN under rare earth ion implantation at medium range energy. Journal Physics D: Applied Physics, 2011, 44, 295402.	1.3	13
318	Optimization Of A Mass Spectrometry Process. , 2011, , .		0
319	A Double Scattering Analytical Model For Elastic Recoil Detection Analysis. , 2011, , .		1
320	Unintentional incorporation of hydrogen in wurtzite InN with different surface orientations. Journal of Applied Physics, 2011, 110, .	1.1	3
321	Zeeman splittings of the <sup>5</sup> D <sub>0</sub> – <sup>7</sup> F <sub>2</sub> transitions of Eu <sup>3+</sup> ions implanted into GaN. Materials Research Society Symposia Proceedings, 2011, 1290, 1.	0.1	6
322	Damage formation in GaN under medium energy range implantation of rare earth ions: a combined TEM, XRD and RBS/C investigation. Materials Research Society Symposia Proceedings, 2011, 1342, 35.	0.1	0
323	Ternary AlGaN Alloys with High Al Content and Enhanced Compositional Homogeneity Grown by Plasma-Assisted Molecular Beam Epitaxy. Japanese Journal of Applied Physics, 2011, 50, 031001.	0.8	9
324	Integration Of SIMS Into A General Purpose IBA Data Analysis Code. AIP Conference Proceedings, 2011, , .	0.3	4

#	Article	IF	CITATIONS
325	Hydrogen In Group-III Nitrides: An Ion Beam Analysis Study. , 2011, , .		1
326	Stopping Power Of He, C And O In InN. , 2011, , .		2
327	N-Doped Photocatalytic Titania Thin Films on Active Polymer Substrates. Journal of Nanoscience and Nanotechnology, 2010, 10, 1072-1077.	0.9	11
328	Crystal Size and Crystalline Volume Fraction Effects on the Erbium Emission of nc-Si:Er Grown by r.f. Sputtering. Journal of Nanoscience and Nanotechnology, 2010, 10, 2663-2668.	0.9	5
329	Influence of Deposition Pressure on N-doped ZnO Films by RF Magnetron Sputtering. Journal of Nanoscience and Nanotechnology, 2010, 10, 2674-2678.	0.9	3
330	Defect studies and optical activation of Yb doped GaN. Journal of Physics: Conference Series, 2010, 249, 012053.	0.3	2
331	Effect of grain size and hydrogen passivation on the electrical properties of nanocrystalline silicon films. International Journal of Materials and Product Technology, 2010, 39, 195.	0.1	5
332	Influence of temperature and plasma composition on deuterium retention in refractory metals. Nuclear Instruments & Methods in Physics Research B, 2010, 268, 2124-2128.	0.6	2
333	Effect of Eu2O3 doping on Ta2O5 crystal growth by the laser-heated pedestal technique. Journal of Crystal Growth, 2010, 313, 62-67.	0.7	7
334	Single and polycrystalline mullite fibres grown by laser floating zone technique. Journal of the European Ceramic Society, 2010, 30, 3311-3318.	2.8	20
335	Multilayers of Ge nanocrystals embedded in Al2O3 matrix: Structural and electrical studies. Microelectronic Engineering, 2010, 87, 2508-2512.	1.1	8
336	Carbon film growth and hydrogenic retention of tungsten exposed to carbon-seeded high density deuterium plasmas. Journal of Nuclear Materials, 2010, 396, 176-180.	1.3	2
337	Stopping power of 11B in Si and TiO2 measured with a bulk sample method and Bayesian inference data analysis. Nuclear Instruments & Methods in Physics Research B, 2010, 268, 1768-1771.	0.6	10
338	High Resolution and Differential PIXE combined with RBS, EBS and AFM analysis of magnesium titanate (MgTiO3) multilayer structures. Nuclear Instruments & Methods in Physics Research B, 2010, 268, 1980-1985.	0.6	20
339	Erosion and re-deposition processes in JET tiles studied with ion beams. Nuclear Instruments & Methods in Physics Research B, 2010, 268, 1991-1996.	0.6	15
340	Effects of Mg-ion implantation in α-Al2O3 and α-Al2O3:Mg crystals: Electrical conductivity and electronic structure changes. Nuclear Instruments & Methods in Physics Research B, 2010, 268, 2874-2877.	0.6	3
341	High temperature annealing of Europium implanted AlN. Nuclear Instruments & Methods in Physics Research B, 2010, 268, 2907-2910.	0.6	4
342	Damage recovery and optical activity in europium implanted wide gap oxides. Nuclear Instruments & Methods in Physics Research B, 2010, 268, 3137-3141.	0.6	5

#	Article	IF	CITATIONS
343	Structural study of Si1â^'xGex nanocrystals embedded in SiO2 films. Thin Solid Films, 2010, 518, 2569-2572.	0.8	9
344	Strain dependence electrical resistance and cohesive strength of ITO thin films deposited on electroactive polymer. Thin Solid Films, 2010, 518, 4525-4528.	0.8	13
345	Room temperature paramagnetism of ZnO:Mn films grown by RF-sputtering. Thin Solid Films, 2010, 518, 4612-4614.	0.8	7
346	Functional and optical properties of Au:TiO2 nanocomposite films: The influence of thermal annealing. Applied Surface Science, 2010, 256, 6536-6542.	3.1	43
347	Al1â^'xInxN/GaN bilayers: Structure, morphology, and optical properties. Physica Status Solidi (B): Basic Research, 2010, 247, 1740-1746.	0.7	10
348	Influence of thermal annealing on the structural and optical properties of GaN/AlN quantum dots. Physica Status Solidi (B): Basic Research, 2010, 247, 1675-1678.	0.7	5
349	Total reflectance and Raman studies in Al <sub>y</sub> In <sub>x</sub> Ga <sub>1â€xâ€y</sub> N epitaxial layers. Physica Status Solidi C: Current Topics in Solid State Physics, 2010, 7, 56-59.	0.8	Ο
350	Erbium-doped nanocrystalline silicon thin films produced by RF sputtering - annealing effect on the Er emission. Physica Status Solidi C: Current Topics in Solid State Physics, 2010, 7, NA-NA.	0.8	2
351	Raman study of dopedâ€ZnO thin films grown by rf sputtering. Physica Status Solidi C: Current Topics in Solid State Physics, 2010, 7, 2290-2293.	0.8	13
352	Growth and characterization of Mnâ€doped ZnO/TiO <sub>2</sub> multilayer nanostructures grown by pulsed laser deposition. Physica Status Solidi C: Current Topics in Solid State Physics, 2010, 7, 2724-2726.	0.8	0
353	Effect of annealing on AlN/GaN quantum dot heterostructures: advanced ion beam characterization and Xâ€ray study of lowâ€dimensional structures. Surface and Interface Analysis, 2010, 42, 1552-1555.	0.8	6
354	The Characterization of N Interstitials and Dangling Bond Point Defects on Ionâ€Implanted GaN Nanowires Studied by Photoluminescence and Xâ€Ray Absorption Spectroscopy. Journal of the American Ceramic Society, 2010, 93, 3531-3534.	1.9	7
355	Electrical and Raman Scattering Studies of ZnO:P and ZnO:Sb Thin Films. Journal of Nanoscience and Nanotechnology, 2010, 10, 2620-2623.	0.9	8
356	Consolidation of Cu-nDiamond Nanocomposites: Hot Extrusion vs Spark Plasma Sintering. Materials Science Forum, 2010, 636-637, 682-687.	0.3	14
357	Hydrogenic retention of high-Z refractory metals exposed to ITER divertor-relevant plasma conditions. Nuclear Fusion, 2010, 50, 055004.	1.6	17
358	High Mobility a-IGO Films Produced at Room Temperature and Their Application in TFTs. Electrochemical and Solid-State Letters, 2010, 13, H20.	2.2	52
359	Defects in Irradiated ZnO Thin Films Studied by Photoluminescence and Photoconductivity. Materials Research Society Symposia Proceedings, 2010, 1268, 1.	0.1	1
360	Functionalizing self-assembled GaN quantum dot superlattices by Eu-implantation. Journal of Applied Physics, 2010, 108, 084306.	1.1	16

#	Article	IF	CITATIONS
361	Hydrogen in InN: A ubiquitous phenomenon in molecular beam epitaxy grown material. Applied Physics Letters, 2010, 96, .	1.5	36
362	Lattice site location of optical centers in GaN:Eu light emitting diode material grown by organometallic vapor phase epitaxy. Applied Physics Letters, 2010, 97, 111911.	1.5	29
363	Optical doping and damage formation in AlN by Eu implantation. Journal of Applied Physics, 2010, 107, 023525.	1.1	38
364	Structural anisotropy of nonpolar and semipolar InN epitaxial layers. Journal of Applied Physics, 2010, 108, .	1.1	21
365	Indium kinetics during the plasma-assisted molecular beam epitaxy of semipolar (11â^22) InGaN layers. Applied Physics Letters, 2010, 96, 181907.	1.5	27
366	lsotopic fingerprints of Pt-containing luminescence centers in highly enrichedS28i. Physical Review B, 2010, 81, .	1.1	10
367	Mn-doped ZnO nanocrystals embedded in Al <sub>2</sub> O <sub>3</sub> : structural and electrical properties. Nanotechnology, 2010, 21, 505705.	1.3	11
368	Optical and Structural Properties of an Eu Implanted Gallium Nitride Quantum Dots/Aluminium Nitride Superlattice. Journal of Nanoscience and Nanotechnology, 2010, 10, 2473-2478.	0.9	3
369	Depth-resolved analysis of spontaneous phase separation in the growth of lattice-matched AlInN. Journal Physics D: Applied Physics, 2010, 43, 055406.	1.3	33
370	Improved Route for the Synthesis of Colloidal NaYF <sub>4</sub> Nanocrystals and Electron Spin Resonance of Gd <sup>3+</sup> Local Probe. Journal of Nanoscience and Nanotechnology, 2010, 10, 5708-5714.	0.9	1
371	Structural and thermal characterization of SiO2–P2O5 sol–gel powders upon annealing at high temperatures. Journal of Non-Crystalline Solids, 2010, 356, 495-501.	1.5	21
372	Identification of the prime optical center in <mml:math xmlns:mml="http://www.w3.org/1998/Math/MathML" display="inline"&gt;<mml:mrow><mml:mtext>GaN</mml:mtext><mml:mo>:</mml:mo><mml:msup><mml:mrow> Physical Review B, 2010, 81, .</mml:mrow></mml:msup></mml:mrow></mml:math 	cmmi:mte	xt>£u
373	RE Implantation and Annealing of III-Nitrides. Topics in Applied Physics, 2010, , 25-54.	0.4	7
374	Computer Control of a 3 MV Van de Graaff Accelerator. Metrology and Measurement Systems, 2010, 17, 415-425.	1.4	0
375	The Structure of Sapphire Implanted with Carbon at Room Temperature and 1000° C. , 2009, , .		1
376	Stopping Power of Different lons in Si Measured with a Bulk Sample Method and Bayesian Inference Data Analysis. , 2009, , .		9
377	Luminescence of Eu ions in <mml:math <br="" xmlns:mml="http://www.w3.org/1998/Math/MathML">display="inline"&gt;<mml:mrow><mml:msub><mml:mrow><mml:mtext>Al</mml:mtext></mml:mrow><mml:mi>x&lt; the entire alloy composition range. Physical Review B, 2009, 80, .</mml:mi></mml:msub></mml:mrow></mml:math>	:/mmal:mi>	<b maml:msub
378	Enhancement in the photocatalytic nature of nitrogen-doped PVD-grown titanium dioxide thin films. Journal of Applied Physics, 2009, 106, .	1.1	37

#	Article	IF	CITATIONS
379	Structural and optical properties of Zn0.9Mn0.1O/ZnO core-shell nanowires designed by pulsed laser deposition. Journal of Applied Physics, 2009, 106, .	1.1	13
380	Optical and structural properties of Eu-implanted InxAl1â^'xN. Journal of Applied Physics, 2009, 106, .	1.1	3
381	Room-Temperature Cosputtered HfO[sub 2]–Al[sub 2]O[sub 3] Multicomponent Gate Dielectrics. Electrochemical and Solid-State Letters, 2009, 12, G65.	2.2	22
382	Structural and optical characterization of Eu-implanted GaN. Journal Physics D: Applied Physics, 2009, 42, 165103.	1.3	48
383	Nanoscale Materials Defect Characterisation. Particle Acceleration and Detection, 2009, , 185-204.	0.3	0
384	Optically active centers in Eu implanted, Euin situdoped GaN, and Eu doped GaN quantum dots. Journal of Applied Physics, 2009, 105, 043104.	1.1	38
385	Breakdown of anomalous channeling with ion energy for accurate strain determination in GaN-based heterostructures. Applied Physics Letters, 2009, 95, 051921.	1.5	5
386	Influence of steering effects on strain detection in AlGaInN/GaN heterostructures by ion channelling. Journal Physics D: Applied Physics, 2009, 42, 065420.	1.3	6
387	Intrinsic <i>p</i> Type ZnO Films Deposited by rf Magnetron Sputtering. Journal of Nanoscience and Nanotechnology, 2009, 9, 813-816.	0.9	7
388	Europium doping of zincblende GaN by ion implantation. Journal of Applied Physics, 2009, 105, 113507.	1.1	8
389	Hydrogenic retention in tungsten exposed to ITER divertor relevant plasma flux densities. Journal of Nuclear Materials, 2009, 390-391, 610-613.	1.3	14
390	Characterisation of titanium beryllides with different microstructure. Fusion Engineering and Design, 2009, 84, 1136-1139.	1.0	12
391	Phase transitions in erbium-doped silicon exposed to laser radiation. Journal of Applied Spectroscopy, 2009, 76, 209-214.	0.3	5
392	Structural and photoluminescence studies of erbiumâ€implanted nanocrystalline silicon thin films. Physica Status Solidi (A) Applications and Materials Science, 2009, 206, 2161-2165.	0.8	0
393	Electrical, structural and optical characterization of copper oxide thin films as a function of post annealing temperature. Physica Status Solidi (A) Applications and Materials Science, 2009, 206, 2143-2148.	0.8	67
394	Temperature behavior of damage in sapphire implanted with light ions. Nuclear Instruments & Methods in Physics Research B, 2009, 267, 1464-1467.	0.6	4
395	Lattice location and annealing studies of Hf implanted CaF2. Nuclear Instruments & Methods in Physics Research B, 2009, 267, 1472-1475.	0.6	1
396	Radiation damage in ZnO ion implanted at 15K. Nuclear Instruments & Methods in Physics Research B, 2009, 267, 2708-2711.	0.6	64

#	Article	IF	CITATIONS
397	Stable In-defect complexes in GaN and AIN. Physica B: Condensed Matter, 2009, 404, 4866-4869.	1.3	4
398	Role of impurities and dislocations for the unintentional n-type conductivity in InN. Physica B: Condensed Matter, 2009, 404, 4476-4481.	1.3	15
399	The role of composition, morphology and crystalline structure in the electrochemical behaviour of TiNx thin films for dry electrode sensor materials. Electrochimica Acta, 2009, 55, 59-67.	2.6	40
400	Structural and electrical properties of Al doped ZnO thin films deposited at room temperature on poly(vinilidene fluoride) substrates. Thin Solid Films, 2009, 517, 6290-6293.	0.8	24
401	Compositional analysis and evolution of defects formed on GaInP epilayers grown on Germanium. Superlattices and Microstructures, 2009, 45, 277-284.	1.4	14
402	Ion beam processing of sapphire single crystals. Surface and Coatings Technology, 2009, 203, 2357-2362.	2.2	9
403	Structural evolution of Ti–Al–Si–N nanocomposite coatings. Vacuum, 2009, 83, 1206-1212.	1.6	36
404	Adhesion failures on hard coatings induced by interface anomalies. Vacuum, 2009, 83, 1213-1217.	1.6	18
405	Structural and optical properties of nitrogen doped ZnO films. Vacuum, 2009, 83, 1274-1278.	1.6	11
406	Influence of the AlN molar fraction on the structural and optical properties of praseodymium-doped AlxGa1â^'xN (0⩽x⩽1) alloys. Microelectronics Journal, 2009, 40, 377-380.	1.1	15
407	Structural and optical properties on thulium-doped LHPG-grown Ta2O5 fibres. Microelectronics Journal, 2009, 40, 309-312.	1.1	10
408	Microstructural evolution in tungsten and copper probes under hydrogen irradiation at ISTTOK. Journal of Nuclear Materials, 2009, 390-391, 1039-1042.	1.3	7
409	Comparison of the damage in sapphire due to implantation of boron, nitrogen, and iron. Journal of Nuclear Materials, 2009, 389, 311-316.	1.3	6
410	Morphological and optical properties of silicon thin films by PLD. Applied Surface Science, 2009, 255, 5299-5302.	3.1	9
411	Photosensitivity of nanocrystalline ZnO films grown by PLD. Applied Surface Science, 2009, 255, 5917-5921.	3.1	9
412	New Approaches to Thermoelectric Materials. NATO Science for Peace and Security Series B: Physics and Biophysics, 2009, , 51-67.	0.2	5
413	Features of the pulsed treatment of silicon layers implanted with erbium ions. Journal of Surface Investigation, 2009, 3, 604-607.	0.1	2
414	Annealing Ni nanocrystalline on WC–Co. Journal of Alloys and Compounds, 2009, 482, 131-136.	2.8	2

#	Article	IF	CITATIONS
415	Free electron behavior in InN: On the role of dislocations and surface electron accumulation. Applied Physics Letters, 2009, 94, 022109.	1.5	41
416	ZrO <sub><i>x</i></sub> N <sub><i>y</i></sub> decorative thin films prepared by the reactive gas pulsing process. Journal Physics D: Applied Physics, 2009, 42, 195501.	1.3	24
417	Electrical properties of sol–gel derived MPB 0.37BiScO3–0.63PbTiO3 thin films deposited on iridium oxide electrodes. Journal of Materials Chemistry, 2009, 19, 5572.	6.7	7
418	Ion Beam Analysis of Iridium-Based TES for Microcalorimeter Detectors. , 2009, , .		0
419	ZnO Thin Films Implanted with Al, Sb and P: Optical, Structural and Electrical Characterization. Journal of Nanoscience and Nanotechnology, 2009, 9, 3574-3577.	0.9	2
420	Box 6: Nanoscale Defects. Particle Acceleration and Detection, 2009, , 205-210.	0.3	0
421	Elemental and RBS analysis of hybrid materials prepared by gamma-irradiation. Nuclear Instruments & Methods in Physics Research B, 2008, 266, 288-294.	0.6	6
422	RBS analysis of InGaN/GaN quantum wells for hybrid structures with efficient Förster coupling. Nuclear Instruments & Methods in Physics Research B, 2008, 266, 1402-1406.	0.6	2
423	Determination of non-Rutherford cross-sections from simple RBS spectra using Bayesian inference data analysis. Nuclear Instruments & Methods in Physics Research B, 2008, 266, 1180-1184.	0.6	12
424	Defect studies on fast and thermal neutron irradiated GaN. Nuclear Instruments & Methods in Physics Research B, 2008, 266, 2780-2783.	0.6	20
425	Anisotropy effects on the formation of new phases in α-Al2O3 by high fluence Zn implantation. Nuclear Instruments & Methods in Physics Research B, 2008, 266, 3129-3132.	0.6	1
426	Mechanisms of AlInN growth by MOVPE: modeling and experimental study. Physica Status Solidi C: Current Topics in Solid State Physics, 2008, 5, 1688-1690.	0.8	8
427	Luminescence and vibrational properties of erbium-implanted nanoporous GaN. Physica Status Solidi C: Current Topics in Solid State Physics, 2008, 5, 1753-1755.	0.8	Ο
428	A comparative investigation of the damage buildâ€up in GaN and Si during rare earth ion implantation. Physica Status Solidi (A) Applications and Materials Science, 2008, 205, 68-70.	0.8	3
429	Rare earth doping of Illâ€nitride alloys by ion implantation. Physica Status Solidi (A) Applications and Materials Science, 2008, 205, 34-37.	0.8	8
430	Role of the oxygen partial pressure on the properties of undoped tin oxide films deposited at low temperature. Physica Status Solidi (A) Applications and Materials Science, 2008, 205, 1957-1960.	0.8	1
431	Luminescence spectroscopy of Euâ€implanted zincblende GaN. Physica Status Solidi (B): Basic Research, 2008, 245, 170-173.	0.7	3
432	Relaxation of compressively strained AlInN on GaN. Journal of Crystal Growth, 2008, 310, 4058-4064.	0.7	50

#	Article	IF	CITATIONS
433	Comparison of ZnO thin films grown by pulsed laser deposition on sapphire and Si substrates. Physica E: Low-Dimensional Systems and Nanostructures, 2008, 40, 699-704.	1.3	19
434	A comparative structural investigation of GaN implanted with rare earth ions at room temperature and 500°C. Materials Science and Engineering B: Solid-State Materials for Advanced Technology, 2008, 146, 204-207.	1.7	9
435	Effect of post-annealing on the properties of copper oxide thin films obtained from the oxidation of evaporated metallic copper. Applied Surface Science, 2008, 254, 3949-3954.	3.1	226
436	Memory effect on CdSe nanocrystals embedded in SiO2 matrix. Solid State Communications, 2008, 148, 105-108.	0.9	11
437	Influence of air oxidation on the properties of decorative NbOxNy coatings prepared by reactive gas pulsing. Surface and Coatings Technology, 2008, 202, 2363-2367.	2.2	16
438	Effect of thermal treatments on the structure of MoNxOy thin films. Vacuum, 2008, 82, 1428-1432.	1.6	18
439	Raman and XRD studies of Ge nanocrystals in alumina films grown by RF-magnetron sputtering. Vacuum, 2008, 82, 1466-1469.	1.6	25
440	PVD-Grown photocatalytic TiO2 thin films on PVDF substrates for sensors and actuators applications. Thin Solid Films, 2008, 517, 1161-1166.	0.8	48
441	Electronic properties of Ge islands embedded in multilayer and superlattice structures. Thin Solid Films, 2008, 517, 303-305.	0.8	2
442	Radiation hardness of GeSi heterostructures with thin Ge layers. Materials Science and Engineering B: Solid-State Materials for Advanced Technology, 2008, 147, 191-194.	1.7	7
443	Ion beam studies of InAs/GaAs self assembled quantum dots. Nuclear Instruments & Methods in Physics Research B, 2008, 266, 1439-1442.	0.6	0
444	Electrical conductivity in undoped $\hat{I}\pm$ -Al2O3 crystals implanted with Mg ions. Nuclear Instruments & Methods in Physics Research B, 2008, 266, 2932-2935.	0.6	6
445	Structural study of the oxidation process and stability of NbOxNy coatings. Nuclear Instruments & Methods in Physics Research B, 2008, 266, 4927-4932.	0.6	1
446	Charging effects in CdSe nanocrystals embedded in SiO2 matrix produced by rf magnetron sputtering. Microelectronic Engineering, 2008, 85, 2374-2377.	1.1	11
447	Visible and infrared luminescence study of Er doped β-Ga <sub>2</sub> O <sub>3</sub> and Er <sub>3</sub> Ga <sub>5</sub> O <sub>12</sub> . Journal Physics D: Applied Physics, 2008, 41, 065406.	1.3	29
448	Influence of the chemical and electronic structure on the electrical behavior of zirconium oxynitride films. Journal of Applied Physics, 2008, 103, .	1.1	66
449	Microwave dielectric permittivity and photoluminescence of Eu2O3 doped laser heated pedestal growth Ta2O5 fibers. Applied Physics Letters, 2008, 92, 252904.	1.5	6
450	Two colour experiments in Eu3+ implanted GaN. Journal of Alloys and Compounds, 2008, 451, 140-142.	2.8	6

#	Article	IF	CITATIONS
451	Evaluation of exposure parameters in plain radiography: a comparative study with European guidelines. Radiation Protection Dosimetry, 2008, 129, 316-320.	0.4	7
452	Co-doping of aluminium and gallium with nitrogen in ZnO films deposited by RF magnetron sputtering. Journal of Physics Condensed Matter, 2008, 20, 075220.	0.7	7
453	Effects of hydrogen permeation on W, Mo and Cu Langmuir probes at ISTTOK. Materials Research Society Symposia Proceedings, 2008, 1125, 1.	0.1	0
454	Microstructure characterization of ODS-RAFM steels. Materials Research Society Symposia Proceedings, 2008, 1125, 1.	0.1	0
455	W-Diamond/Cu-Diamond nanostructured composites for fusion devices. Materials Research Society Symposia Proceedings, 2008, 1125, 1.	0.1	1
456	Optical energies of AlInN epilayers. Journal of Applied Physics, 2008, 103, .	1.1	58
457	Further insight into the temperature quenching of photoluminescence from InAsâ^•GaAs self-assembled quantum dots. Journal of Applied Physics, 2008, 103, .	1.1	22
458	Enhancement of Erbium Incorporation with Implantation into Nanoporous GaN. , 2008, , .		0
459	Temperature dependence of the electric field gradient in GaN measured with the PAC-probe 181Hf. , 2008, , 217-223.		Ο
460	OPTICAL AND STRUCTURAL ANALYSIS OF Ge/Si QUANTUM DOTS GROWN ON A Si(001) SURFACE COVERED WITH A SiO2 SUB-MONOLAYER. International Journal of Nanoscience, 2007, 06, 245-248.	0.4	0
461	Metal-organic vapor phase epitaxy and properties of AlInN in the whole compositional range. Applied Physics Letters, 2007, 90, 022105.	1.5	119
462	Arsenic in ZnO and GaN: Substitutional Cation or Anion Sites?. Materials Research Society Symposia Proceedings, 2007, 994, 1.	0.1	2
463	Structural and Oxidation Studies of Titanium Beryllides. Nuclear Technology, 2007, 159, 233-237.	0.7	2
464	Tribological behaviour of Cl-implanted TiN coatings for biomedical applications. Wear, 2007, 262, 1337-1345.	1.5	28
465	Efficient dipole-dipole coupling of Mott-Wannier and Frenkel excitons in (Ga,In)N quantum well/polyfluorene semiconductor heterostructures. Physical Review B, 2007, 76, .	1.1	64
466	Stability of GaN films under intense MeV He ion irradiation. Diamond and Related Materials, 2007, 16, 1437-1440.	1.8	3
467	Structural and optical properties of Er3+ion in sol–gel grown LiNbO3. Journal of Physics Condensed Matter, 2007, 19, 016213.	0.7	8
468	Role of Nanoscale Strain Inhomogeneity on the Light Emission from InGaN Epilayers. Advanced Functional Materials, 2007, 17, 37-42.	7.8	60

#	Article	IF	CITATIONS
469	Lattice location of implanted As in ZnO. Superlattices and Microstructures, 2007, 42, 8-13.	1.4	4
470	Optical and structural behaviour of Cu-implanted sapphire. Surface and Coatings Technology, 2007, 201, 8190-8196.	2.2	9
471	Influence of the O/C ratio in the behaviour of TiCxOy thin films. Surface and Coatings Technology, 2007, 201, 5587-5591.	2.2	28
472	Dual DC magnetron cathode co-deposition of (Al,Ti) and (Al,Ti,N) thin films with controlled depth composition. Vacuum, 2007, 81, 1503-1506.	1.6	4
473	Microstructural studies and electrical properties of Mg-doped SrTiO3 thin films. Acta Materialia, 2007, 55, 4947-4954.	3.8	9
474	Influence of the sol–gel growth parameters on the optical and structural properties on LiNbO3 samples. Materials Science and Engineering C, 2007, 27, 1065-1068.	3.8	4
475	Structural and optical characterisation of Eu implanted AlxGa1â^'xN. Nuclear Instruments & Methods in Physics Research B, 2007, 257, 307-310.	0.6	10
476	Implantation of nanoporous GaN with Eu ions. Nuclear Instruments & Methods in Physics Research B, 2007, 257, 328-331.	0.6	2
477	Synthesis of ZnO nanocrystals in sapphire by ion implantation and vacuum annealing. Nuclear Instruments & Methods in Physics Research B, 2007, 257, 515-518.	0.6	14
478	Lithium ion implantation and annealing of MgO single crystals. Nuclear Instruments & Methods in Physics Research B, 2007, 257, 558-562.	0.6	1
479	Copper and cobalt nanocolloids in implanted MgO crystals. Nuclear Instruments & Methods in Physics Research B, 2007, 257, 563-567.	0.6	7
480	Spectroscopic investigation of implanted epilayers of Tm3+:GaN. Journal of Luminescence, 2007, 122-123, 131-133.	1.5	3
481	Radiation-induced structural transformations in a silicon layer of SOI. Physica Status Solidi (A) Applications and Materials Science, 2007, 204, 2645-2650.	0.8	1
482	Relaxation behaviour of Co and Ni implanted into MgO. Journal of Magnetism and Magnetic Materials, 2007, 316, e776-e778.	1.0	6
483	Anisotropic ferromagnetism induced in rutile single crystals by Co implantation. European Physical Journal B, 2007, 55, 253-260.	0.6	15
484	Optical studies of ZnO nanocrystals doped with Eu3+ ions. Applied Physics A: Materials Science and Processing, 2007, 88, 129-133.	1.1	53
485	Temperature dependence of the electric field gradient in GaN measured with the PAC-probe 181Hf. Hyperfine Interactions, 2007, 177, 89-95.	0.2	5
486	Holistic RBS–PIXE data reanalysis of SBT thin film samples. Nuclear Instruments & Methods in Physics Research B, 2007, 261, 439-442.	0.6	11

#	Article	IF	CITATIONS
487	Ion implantation and ion beam analysis of MOD deposited oxide films. Nuclear Instruments & Methods in Physics Research B, 2007, 261, 456-460.	0.6	0
488	Synthesis, surface modification and optical properties of Tb3+-doped ZnO nanocrystals. Nanotechnology, 2006, 17, 834-839.	1.3	75
489	Anomalous Ion Channeling inAlInN/GaNBilayers: Determination of the Strain State. Physical Review Letters, 2006, 97, 085501.	2.9	125
490	Study of the oxygen role in the photoluminescence of erbium doped nanocrystalline silicon embedded in a silicon amorphous matrix. Journal of Non-Crystalline Solids, 2006, 352, 1148-1151.	1.5	2
491	Optical active centres in ZnO samples. Journal of Non-Crystalline Solids, 2006, 352, 1453-1456.	1.5	18
492	Radiation-induced defects in a-Si:H by 1.5MeV He4 particles studied by photoconductivity and photothermal deflection spectroscopy. Journal of Non-Crystalline Solids, 2006, 352, 1071-1074.	1.5	6
493	Hydrogenated silicon carbon nitride films obtained by HWCVD, PA-HWCVD and PECVD techniques. Journal of Non-Crystalline Solids, 2006, 352, 1361-1366.	1.5	45
494	Transparent thin film transistors based on indium oxide semiconductor. Journal of Non-Crystalline Solids, 2006, 352, 2311-2314.	1.5	48
495	Optical properties of Er3++ Yb3+doped gallium nitride layers. , 2006, , .		Ο
496	Luminescence and structural properties of defects in ion implanted ZnO. Physica Status Solidi C: Current Topics in Solid State Physics, 2006, 3, 968-971.	0.8	9
497	Investigations of p-type signal for ZnO thin films grown on (100) GaAs substrates by pulsed laser deposition. Physica Status Solidi C: Current Topics in Solid State Physics, 2006, 3, 1038-1041.	0.8	16
498	Depth profiling of ion-implanted AlInN using time-of-flight secondary ion mass spectrometry and cathodoluminescence. Physica Status Solidi C: Current Topics in Solid State Physics, 2006, 3, 1927-1930.	0.8	8
499	Behaviour of the AlN cap during GaN implantation of rare earths and annealing. Physica Status Solidi (A) Applications and Materials Science, 2006, 203, 2172-2175.	0.8	8
500	Structure and role of ultrathin AlN layers for improving optical activation of rare earth implanted GaN. Physica Status Solidi (B): Basic Research, 2006, 243, 1541-1544.	0.7	1
501	Investigation of the nonlinear optical characteristics of composite materials based on sapphire with silver, copper, and gold nanoparticles by the reflection Z-scan method. Optics and Spectroscopy (English Translation of Optika I Spektroskopiya), 2006, 101, 615-622.	0.2	11
502	Microstructural studies of PZT thick films on Cu foils. Acta Materialia, 2006, 54, 3211-3220.	3.8	24
503	Optical doping of AlN by rare earth implantation. Nuclear Instruments & Methods in Physics Research B, 2006, 242, 307-310.	0.6	23
504	Optical properties tailoring by high fluence implantation of Ag ions on sapphire. Nuclear Instruments & Methods in Physics Research B, 2006, 242, 104-108.	0.6	9

#	Article	IF	CITATIONS
505	Stability and luminescence studies of Tm and Er implanted ZnO single crystals. Nuclear Instruments & Methods in Physics Research B, 2006, 242, 580-584.	0.6	25
506	Accurate simulation of backscattering spectra in the presence of sharp resonances. Nuclear Instruments & Methods in Physics Research B, 2006, 247, 381-389.	0.6	23
507	Compositional and structural changes in ZrOxNy films depending on growth condition. Nuclear Instruments & Methods in Physics Research B, 2006, 249, 458-461.	0.6	8
508	RBS/channeling study of buried Ge quantum dots grown in a Si layer. Nuclear Instruments & Methods in Physics Research B, 2006, 249, 462-465.	0.6	5
509	Ion beam characterisation of ODS steel samples after long term annealing conditions. Nuclear Instruments & Methods in Physics Research B, 2006, 249, 493-496.	0.6	6
510	RBS and XRD analysis of SiGe/Ge heterostructures for p-HMOS applications. Nuclear Instruments & Methods in Physics Research B, 2006, 249, 878-881.	0.6	0
511	Defect production in neutron irradiated GaN. Nuclear Instruments & Methods in Physics Research B, 2006, 249, 358-361.	0.6	27
512	Structure and optical properties of sapphire implanted with boron at room temperature and 1000°C. Nuclear Instruments & Methods in Physics Research B, 2006, 250, 81-84.	0.6	3
513	Optical and structural behaviour of Mn implanted sapphire. Nuclear Instruments & Methods in Physics Research B, 2006, 250, 90-94.	0.6	1
514	TEM investigation of Tm implanted GaN, the influence of high temperature annealing. Optical Materials, 2006, 28, 738-741.	1.7	16
515	High temperature annealing of rare earth implanted GaN films: Structural and optical properties. Optical Materials, 2006, 28, 750-758.	1.7	47
516	Lattice order in thulium-doped GaN epilayers: In situ doping versus ion implantation. Optical Materials, 2006, 28, 771-774.	1.7	6
517	Effect of annealing temperature on luminescence in Eu implanted GaN. Optical Materials, 2006, 28, 780-784.	1.7	29
518	Influence of defects on the optical and structural properties of Ge dots embedded in an Si/Ge superlattice. Journal of Luminescence, 2006, 121, 417-420.	1.5	11
519	Simulation of deep resonances in elastic backscattering data. Nuclear Instruments & Methods in Physics Research B, 2006, 249, 796-799.	0.6	2
520	Analysis of sol–gel silica–titania films doped with Ag and Er using artificial neural networks. Nuclear Instruments & Methods in Physics Research B, 2006, 249, 804-807.	0.6	3
521	Damage behaviour of GaAs/AlAs multilayer structures. Nuclear Instruments & Methods in Physics Research B, 2006, 249, 890-893.	0.6	1
522	Optical behaviour of Er doped rutile by ion implantation. Nuclear Instruments & Methods in Physics Research B, 2006, 250, 363-367.	0.6	4

#	Article	IF	CITATIONS
523	Lattice sites of implanted Cu and Ag in ZnO. Superlattices and Microstructures, 2006, 39, 229-237.	1.4	20
524	The structure of crystallographic damage in GaN formed during rare earth ion implantation with and without an ultrathin AlN capping layer. Superlattices and Microstructures, 2006, 40, 300-305.	1.4	4
525	Blue cathodoluminescence from thulium implanted AlxGa1â^'xN and InxAl1â^'xN. Superlattices and Microstructures, 2006, 40, 445-451.	1.4	10
526	Optical studies on a coherent InGaN/GaN layer. Superlattices and Microstructures, 2006, 40, 452-457.	1.4	2
527	Structural evolution in ZrNxOy thin films as a function of temperature. Surface and Coatings Technology, 2006, 200, 2917-2922.	2.2	46
528	Tribocorrosion behaviour of ZrOxNy thin films for decorative applications. Surface and Coatings Technology, 2006, 200, 6634-6639.	2.2	32
529	Diffusion processes in seeded and unseeded SBT thin films with varied stoichiometry. Surface Science, 2006, 600, 1780-1786.	0.8	11
530	Properties of MoNxOy thin films as a function of the N/O ratio. Thin Solid Films, 2006, 494, 201-206.	0.8	22
531	Ion synthesis and optical properties of gold nanoparticles in an Al2O3 matrix. Technical Physics, 2006, 51, 1474-1481.	0.2	10
532	Optical properties of high-temperature annealed Eu-implanted GaN. Optical Materials, 2006, 28, 797-801.	1.7	8
533	Optical and structural analysis of bulk ZnO samples undoped and rare earth doped by ion implantation. Superlattices and Microstructures, 2006, 39, 202-210.	1.4	25
534	UV-Raman scattering study of lattice recovery by thermal annealing of Eu+ -implanted GaN layers. Superlattices and Microstructures, 2006, 40, 440-444.	1.4	1
535	Optical and structural studies in Eu-implanted AlN films. Superlattices and Microstructures, 2006, 40, 537-544.	1.4	14
536	Raman spectra and structural analysis in ZrOxNy thin films. Thin Solid Films, 2006, 515, 1132-1137.	0.8	38
537	Phase Separation on GalnAsSb Films for Thermophotovoltaic Devices. Materials Science Forum, 2006, 514-516, 447-451.	0.3	1
538	Structural and Optical Characterization of Light Emitting InGaN/GaN Epitaxial Layers. Materials Science Forum, 2006, 514-516, 38-42.	0.3	3
539	Characterization of Nickel Implanted α-Al <sub>2</sub> O <sub>3</sub> . Materials Science Forum, 2006, 514-516, 348-352.	0.3	0
540	X-Ray Diffraction Study of Ordered Antiferromagnets for Tunnel Junctions. Materials Science Forum, 2006, 514-516, 314-318.	0.3	0

#	Article	IF	CITATIONS
541	Ion Beam Analysis of Ge/Si Dots Grown on Ultrathin SiO <sub>2</sub> Interlayers. Materials Science Forum, 2006, 514-516, 1121-1124.	0.3	0
542	Hardware and Software Improvements in the Hotbird. Materials Science Forum, 2006, 514-516, 1678-1681.	0.3	1
543	Phase Transformation and Structural Studies of EUROFER RAFM Alloy. Materials Science Forum, 2006, 514-516, 500-504.	0.3	19
544	Effect of the Matrix on the 1.51¼m Photoluminescence of Er-Doped Silicon Quantum Dots. Materials Science Forum, 2006, 514-516, 1116-1120.	0.3	1
545	Combination of IBA Techniques for Composition Analysis of GaInAsSb Films. Materials Science Forum, 2006, 514-516, 1603-1607.	0.3	5
546	Influence of Rapid Thermal Annealing on the Luminescence Properties of Nanoporous GaN Films. Electrochemical and Solid-State Letters, 2006, 9, G150.	2.2	11
547	Identification of donor-related impurities in ZnO using photoluminescence and radiotracer techniques. Physical Review B, 2006, 73, .	1.1	59
548	Optical activation of Eu ions in nanoporous GaN films. Journal of Applied Physics, 2006, 99, 104305.	1.1	6
549	Cathodoluminescence of rare earth implanted AlInN. Applied Physics Letters, 2006, 89, 131912.	1.5	15
550	Failure mechanism of AlN nanocaps used to protect rare earth-implanted GaN during high temperature annealing. Applied Physics Letters, 2006, 88, 031902.	1.5	18
551	Transmission electron microscopy investigation of the structural damage formed in GaN by medium range energy rare earth ion implantation. Journal of Applied Physics, 2006, 100, 073520.	1.1	58
552	Rare Earth Ion Implantation in GaN: Damage Formation and Recovery. Acta Physica Polonica A, 2006, 110, 125-137.	0.2	3
553	Characterization of the blue emission of Tm/Er co-implanted GaN. Materials Research Society Symposia Proceedings, 2005, 892, 544.	0.1	3
554	Structural and composition analysis of GaN films deposited by cyclic-PLD at different substrate temperatures. Sensors and Actuators A: Physical, 2005, 121, 131-135.	2.0	4
555	XRD analysis of strained Ge–SiGe heterostructures on relaxed SiGe graded buffers grown by hybrid epitaxy on Si(001) substrates. Materials Science and Engineering B: Solid-State Materials for Advanced Technology, 2005, 124-125, 123-126.	1.7	4
556	Stability of erbium and silver implanted in silica–titania sol–gel films. Nuclear Instruments & Methods in Physics Research B, 2005, 240, 415-419.	0.6	4
557	Rutherford backscattering and X-ray reflectivity analysis of tunnel barriers. Nuclear Instruments & Methods in Physics Research B, 2005, 240, 365-370.	0.6	1
558	Analysis of nanolayered samples with a 4He beam. Nuclear Instruments & Methods in Physics Research B, 2005, 241, 361-364.	0.6	0

#	Article	IF	CITATIONS
559	Application of RZ-scan technique for investigation of nonlinear refraction of sapphire doped with Ag, Cu, and Au nanoparticles. Optics Communications, 2005, 253, 205-213.	1.0	58
560	Microstructural characterization of Eurofer-ODS RAFM steel in the normalized and tempered condition and after thermal aging in simulated fusion conditions. Fusion Engineering and Design, 2005, 75-79, 1061-1065.	1.0	21
561	Optical and structural study of Ge/Si quantum dots on Si(100) surface covered with a thin silicon oxide layer. Materials Science and Engineering B: Solid-State Materials for Advanced Technology, 2005, 124-125, 462-465.	1.7	6
562	Compositional and structural characterisation of GaSb and GaInSb. Nuclear Instruments & Methods in Physics Research B, 2005, 240, 360-364.	0.6	3
563	Site location and optical properties of Eu implanted sapphire. Nuclear Instruments & Methods in Physics Research B, 2005, 240, 409-414.	0.6	0
564	Beyond single scattering off flat samples. Nuclear Instruments & Methods in Physics Research B, 2005, 241, 316-320.	0.6	4
565	Ion beam analysis of GalnAsSb films grown by MOVPE on GaSb. Nuclear Instruments & Methods in Physics Research B, 2005, 241, 326-330.	0.6	6
566	High resolution backscattering studies of nanostructured magnetic and semiconducting materials. Nuclear Instruments & Methods in Physics Research B, 2005, 241, 454-458.	0.6	13
567	Characterization of silicon carbide thin films and their use in colour sensor. Solar Energy Materials and Solar Cells, 2005, 87, 343-348.	3.0	2
568	Influence of nitrogen content on the structural, mechanical and electrical properties of TiN thin films. Surface and Coatings Technology, 2005, 191, 317-323.	2.2	146
569	Structural stability of decorative ZrNxOy thin films. Surface and Coatings Technology, 2005, 200, 748-752.	2.2	27
570	Magnetic nanoscale aggregates of cobalt and nickel in MgO single crystals. European Physical Journal B, 2005, 45, 331-338.	0.6	15
571	Nonlinear optical properties of gold nanoparticles synthesized by ion implantation in sapphire matrix. Technical Physics Letters, 2005, 31, 702-705.	0.2	21
572	Magnetic properties of TiO2 rutile implanted with Ni and Co. Journal of Magnetism and Magnetic Materials, 2005, 294, e73-e76.	1.0	20
573	Characterization and stability studies of titanium beryllides. Fusion Engineering and Design, 2005, 75-79, 759-763.	1.0	2
574	The atomic structure of defects formed during doping of GaN with rare earth ions. Physica Status Solidi C: Current Topics in Solid State Physics, 2005, 2, 1081-1084.	0.8	5
575	Detection angle resolved PIXE and the equivalent depth concept for thin film characterization. X-Ray Spectrometry, 2005, 34, 372-375.	0.9	23
576	Influence of the Annealing Ambient on Structural and Optical Properties of Rare Earth Implanted GaN. Materials Research Society Symposia Proceedings, 2005, 892, 556.	0.1	2

#	Article	IF	CITATIONS
577	Annealing properties of ZnO films grown using diethyl zinc and tertiary butanol. Journal of Physics Condensed Matter, 2005, 17, 1719-1724.	0.7	16
578	Comment on "Direct evidence of nanocluster-induced luminescence in InGaN epifilms―[Appl. Phys. Lett. 86, 021911 (2005)]. Applied Physics Letters, 2005, 87, 136101.	1.5	3
579	Up conversion from visible to ultraviolet in bulk ZnO implanted with Tm ions. Applied Physics Letters, 2005, 87, 192108.	1.5	25
580	Damage formation and annealing at low temperatures in ion implanted ZnO. Applied Physics Letters, 2005, 87, 191904.	1.5	100
581	Selectively excited photoluminescence from Eu-implanted GaN. Applied Physics Letters, 2005, 87, 112107.	1.5	85
582	Direct Evidence for As as a Zn-Site Impurity in ZnO. Physical Review Letters, 2005, 95, 215503.	2.9	86
583	A microspectroscopic study of cap damage in annealed RE-doped AlN-capped GaN. Materials Research Society Symposia Proceedings, 2005, 892, 568.	0.1	0
584	A green-emitting CdSe/poly(butyl acrylate) nanocomposite. Nanotechnology, 2005, 16, 1969-1973.	1.3	25
585	Near-band-edge slow luminescence in nominally undoped bulk ZnO. Journal of Applied Physics, 2005, 98, 013502.	1.1	54
586	Structural, electrical, optical, and mechanical characterizations of decorative ZrOxNy thin films. Journal of Applied Physics, 2005, 98, 023715.	1.1	87
587	Recent Emission Channeling Studies in Wide Band Gap Semiconductors. , 2005, , 792-801.		Ο
588	PAC Studies of Implanted 111Ag in Single-Crystalline ZnO. , 2005, , 395-400.		0
589	Lattice location and stability of implanted Cu in ZnO. Physical Review B, 2004, 69, .	1.1	40
590	Exchange bias of MnPt/CoFe films prepared by ion beam deposition. Journal of Applied Physics, 2004, 95, 6317-6321.	1.1	16
591	Direct evidence for strain inhomogeneity in InxGa1â^'xN epilayers by Raman spectroscopy. Applied Physics Letters, 2004, 85, 2235-2237.	1.5	21
592	Influence of O and C co-implantation on the lattice site of Er in GaN. Applied Physics Letters, 2004, 84, 4304-4306.	1.5	15
593	Optical and mechanical properties of MgO crystals implanted with lithium ions. Journal of Applied Physics, 2004, 95, 2371-2378.	1.1	7
594	High-temperature annealing and optical activation of Eu-implanted GaN. Applied Physics Letters, 2004, 85, 2712-2714.	1.5	67

#	Article	IF	CITATIONS
595	The role of microstructure in luminescent properties of Er-doped nanocrystalline Si thin films. Physics of the Solid State, 2004, 46, 113-117.	0.2	2
596	Roughness in GaN/InGaN films and multilayers determined with Rutherford backscattering. Nuclear Instruments & Methods in Physics Research B, 2004, 217, 479-497.	0.6	30
597	Optical changes induced by high fluence implantation of Au ions on sapphire. Nuclear Instruments & Methods in Physics Research B, 2004, 218, 139-144.	0.6	15
598	Stability and optical activity of Er implanted MgO. Nuclear Instruments & Methods in Physics Research B, 2004, 218, 128-132.	0.6	1
599	Defect production in nitrogen implanted sapphire. Nuclear Instruments & Methods in Physics Research B, 2004, 218, 222-226.	0.6	6
600	Comparative study of radiation damage in GaN and InGaN by 400 keV Au implantation. Nuclear Instruments & Methods in Physics Research B, 2004, 218, 36-41.	0.6	28
601	Copper nanocolloids in MgO crystals implanted with Cu ions. Nuclear Instruments & Methods in Physics Research B, 2004, 218, 148-152.	0.6	7
602	Electrical conductivity of as-grown and oxidized MgO:Li crystals implanted with Li ions. Nuclear Instruments & Methods in Physics Research B, 2004, 218, 164-169.	0.6	6
603	The effect of temperature on the structure of iron-implanted sapphire. Nuclear Instruments & Methods in Physics Research B, 2004, 218, 227-231.	0.6	5
604	Characterization of FePt nanoparticles in FePt/C multilayers. Nuclear Instruments & Methods in Physics Research B, 2004, 219-220, 919-922.	0.6	4
605	Study of silica–titania films doped with Er and Ag by RBS and ERDA. Nuclear Instruments & Methods in Physics Research B, 2004, 219-220, 923-927.	0.6	5
606	RBS analysis of AlGaSb thin films. Nuclear Instruments & Methods in Physics Research B, 2004, 219-220, 928-932.	0.6	1
607	Ion beam studies of single crystalline manganite thin films. Nuclear Instruments & Methods in Physics Research B, 2004, 219-220, 933-937.	0.6	0
608	Structural, optical and mechanical properties of coloured TiNxOy thin films. Thin Solid Films, 2004, 447-448, 449-454.	0.8	169
609	Compositional Profiles in Silica-Based Sol-Gel Films Doped with Erbium and Silver, by RBS and ERDA. Journal of Sol-Gel Science and Technology, 2004, 31, 287-291.	1.1	7
610	Amorphisation of GaN during processing with rare earth ion beams. Superlattices and Microstructures, 2004, 36, 737-745.	1.4	27
611	PAC Studies of Implanted 111Ag in Single-Crystalline ZnO. Hyperfine Interactions, 2004, 158, 395-400.	0.2	9
612	Recent Emission Channeling Studies in Wide Band Gap Semiconductors. Hyperfine Interactions, 2004, 159, 363-372.	0.2	9

35

#	Article	IF	CITATIONS
613	Optical and RBS studies in Tm implanted ZnO samples. Physica Status Solidi C: Current Topics in Solid State Physics, 2004, 1, 254-256.	0.8	9
614	Property change in ZrNxOy thin films: effect of the oxygen fraction and bias voltage. Thin Solid Films, 2004, 469-470, 11-17.	0.8	65
615	Corrosion resistance of ZrNxOy thin films obtained by rf reactive magnetron sputtering. Thin Solid Films, 2004, 469-470, 274-281.	0.8	52
616	Optical studies on the red luminescence of InGaN epilayers. Superlattices and Microstructures, 2004, 36, 625-632.	1.4	8
617	Characterisation of defects in rare earth implanted GaN by deep level transient spectroscopy. Superlattices and Microstructures, 2004, 36, 713-719.	1.4	6
618	Extended X-ray absorption fine structure studies of thulium doped GaN epilayers. Superlattices and Microstructures, 2004, 36, 729-736.	1.4	9
619	PL studies on ZnO single crystals implanted with thulium ions. Superlattices and Microstructures, 2004, 36, 747-753.	1.4	14
620	Microstructure of (Ti,Si,Al)N nanocomposite coatings. Surface and Coatings Technology, 2004, 177-178, 369-375.	2.2	52
621	Structural and corrosion behaviour of stoichiometric and substoichiometric TiN thin films. Surface and Coatings Technology, 2004, 180-181, 158-163.	2.2	38
622	Ion beam studies of TiNxOy thin films deposited by reactive magnetron sputtering. Surface and Coatings Technology, 2004, 180-181, 372-376.	2.2	36
623	Atomic environment and interfacial structural order of TiAlN/Mo multilayers. Surface and Coatings Technology, 2004, 187, 393-398.	2.2	10
624	Characterization of hard DC-sputtered Si-based TiN coatings: the effect of composition and ion bombardment. Surface and Coatings Technology, 2004, 188-189, 351-357.	2.2	36
625	Magnetic behavior of Co and Ni implanted MgO. Journal of Magnetism and Magnetic Materials, 2004, 272-276, 840-842.	1.0	11
626	Materials design data for reduced activation martensitic steel type EUROFER. Journal of Nuclear Materials, 2004, 329-333, 257-262.	1.3	118
627	Methods for the mitigation of the chemical reactivity of beryllium in steam. Journal of Nuclear Materials, 2004, 329-333, 1353-1356.	1.3	1
628	Li ceramic pebbles chemical compatibility with Eurofer samples in fusion relevant conditions. Journal of Nuclear Materials, 2004, 329-333, 1295-1299.	1.3	9
629	Lattice location and thermal stability of implanted Fe in ZnO. Applied Physics Letters, 2004, 85, 4899-4901.	1.5	50
630	Degradation of particle detectors based on a-Si:H by 1.5 Mev He4 and 1 MeV protons. Journal of Non-Crystalline Solids, 2004, 338-340, 814-817.	1.5	4

#	Article	IF	CITATIONS
631	Formation of AlxGa1â^'xSb films over GaSb substrates by Al diffusion. EPJ Applied Physics, 2004, 27, 423-426.	0.3	3
632	Lattice site and stability of implanted Ag in ZnO. Physica B: Condensed Matter, 2003, 340-342, 240-244.	1.3	23
633	Lattice location and optical activation of rare earth implanted GaN. Materials Science and Engineering B: Solid-State Materials for Advanced Technology, 2003, 105, 132-140.	1.7	44
634	Structural and optical studies of Co and Ti implanted sapphire. Nuclear Instruments & Methods in Physics Research B, 2003, 207, 55-62.	0.6	10
635	Radiation-damage recovery in undoped and oxidized Li doped MgO crystals implanted with lithium ions. Nuclear Instruments & Methods in Physics Research B, 2003, 206, 148-152.	0.6	6
636	Three-step amorphisation process in ion-implanted GaN at 15 K. Nuclear Instruments & Methods in Physics Research B, 2003, 206, 1028-1032.	0.6	71
637	Annealing behavior and lattice site location of Er implanted InGaN. Nuclear Instruments & Methods in Physics Research B, 2003, 206, 1042-1046.	0.6	3
638	Lattice site location and optical activity of Er implanted ZnO. Nuclear Instruments & Methods in Physics Research B, 2003, 206, 1047-1051.	0.6	66
639	High temperature chemical compatibility between SiC composites and Be pebbles. Nuclear Instruments & Methods in Physics Research B, 2003, 210, 495-500.	0.6	0
640	Implantation and annealing studies of Tm-implanted GaN. Materials Science and Engineering B: Solid-State Materials for Advanced Technology, 2003, 105, 97-100.	1.7	13
641	Optical absorption of a Li-related impurity in ZnO. Physica B: Condensed Matter, 2003, 340-342, 225-229.	1.3	10
642	Optical doping of ZnO with Tm by ion implantation. Physica B: Condensed Matter, 2003, 340-342, 235-239.	1.3	30
643	Influence of crystals distribution on the photoluminescence properties of nanocrystalline silicon thin films. Microelectronics Journal, 2003, 34, 375-378.	1.1	1
644	Effects of the morphology and structure on the elastic behavior of (Ti,Si,Al)N nanocomposites. Surface and Coatings Technology, 2003, 174-175, 984-991.	2.2	21
645	Preparation of magnetron sputtered TiNxOy thin films. Surface and Coatings Technology, 2003, 174-175, 197-203.	2.2	74
646	Mechanical characterization of reactively magnetron-sputtered TiN films. Surface and Coatings Technology, 2003, 174-175, 375-382.	2.2	44
647	Structural characterisation of SiC/SiCf composites exposed to chemical interaction with Be at high temperature. Fusion Engineering and Design, 2003, 69, 221-226.	1.0	0
648	Influence of ionizing radiation on the electrical behavior of a Be pebble bed. Fusion Engineering and Design, 2003, 69, 253-256.	1.0	1

#	Article	IF	CITATIONS
649	Interrelation between microstructure and optical properties of erbium-doped nanocrystalline thin films. Physica E: Low-Dimensional Systems and Nanostructures, 2003, 16, 414-419.	1.3	7
650	Magnetic characterization of U/Co multilayers. Physica Status Solidi A, 2003, 196, 153-156.	1.7	2
651	Degradation of Structural and Optical Properties of InGaN/GaN Multiple Quantum Wells with Increasing Number of Wells. Physica Status Solidi C: Current Topics in Solid State Physics, 2003, 0, 302-306.	0.8	4
652	Analysis of Strain Depth Variations in an In0.19Ga0.81N Layer by Raman Spectroscopy. Physica Status Solidi C: Current Topics in Solid State Physics, 2003, 0, 563-567.	0.8	7
653	Implantation site of rare earths in single-crystalline ZnO. Applied Physics Letters, 2003, 82, 1173-1175.	1.5	55
654	Dielectric function of nanocrystalline silicon with few nanometers (<3 nm) grain size. Applied Physics Letters, 2003, 82, 2993-2995.	1.5	58
655	Photoluminescence and damage recovery studies in Fe-implanted ZnO single crystals. Journal of Applied Physics, 2003, 93, 8995-9000.	1.1	56
656	The influence ofin situphotoexcitation on a defect structure generation in ArÂimplanted GaAs(001) crystals revealed by high-resolution x-ray diffraction and Rutherford backscattering spectroscopy. Journal Physics D: Applied Physics, 2003, 36, A143-A147.	1.3	9
657	Raman study of the A1(LO) phonon in relaxed and pseudomorphic InGaN epilayers. Applied Physics Letters, 2003, 83, 4761-4763.	1.5	53
658	Processing of rare earth doped GaN with ion beams. Materials Research Society Symposia Proceedings, 2003, 798, 569.	0.1	5
659	High Temperature Implantation of Tm in GaN. Materials Research Society Symposia Proceedings, 2003, 798, 548.	0.1	6
660	Electron micro-probe analysis and cathodoluminescence spectroscopy of rare earth - implanted GaN. Materials Research Society Symposia Proceedings, 2003, 798, 466.	0.1	1
661	Room-temperature growth of crystalline indium tin oxide films on glass using low-energy oxygen-ion-beam assisted deposition. Journal of Applied Physics, 2003, 93, 2262-2266.	1.1	42
662	Structural Development in Hard Si-Based TiN Coatings as a Function of Temperature: A Comprehensive Study in Vacuum and in Air. Materials Science Forum, 2002, 383, 151-160.	0.3	2
663	Optical activity and damage recovery of erbium implanted strontium titanate. Radiation Effects and Defects in Solids, 2002, 157, 1071-1076.	0.4	5
664	Depth profiling InGaN/GaN multiple quantum wells by Rutherford backscattering: The role of intermixing. Applied Physics Letters, 2002, 81, 2950-2952.	1.5	15
665	Mechanical and Adhesion Behaviours of Superhard (Ti,Si,Al)N Nanocomposite Films Grown by Reactive Magnetron Sputtering. Key Engineering Materials, 2002, 230-232, 185-188.	0.4	0
666	Lattice Site Location Studies of Rare-Earths Implanted in ZnO Single-Crystals. Materials Research Society Symposia Proceedings, 2002, 744, 1.	0.1	0

#	Article	IF	CITATIONS
667	Structural and optical properties of InGaN/GaN layers close to the critical layer thickness. Applied Physics Letters, 2002, 81, 1207-1209.	1.5	94
668	Strain and composition distributions in wurtzite InGaN/GaN layers extracted from x-ray reciprocal space mapping. Applied Physics Letters, 2002, 80, 3913-3915.	1.5	209
669	Preliminary investigations of infrared Er-related photoluminescence in ion-implanted In0.07Ga0.93N. Applied Physics Letters, 2002, 80, 4504-4506.	1.5	6
670	Luminescence studies of Co implanted sapphires. Radiation Effects and Defects in Solids, 2002, 157, 1117-1122.	0.4	1
671	Ion beam studies of MBE grown GaN films on silicon substrates. Nuclear Instruments & Methods in Physics Research B, 2002, 188, 73-77.	0.6	6
672	Study of roughness in Ti0.4Al0.6N/Mo multilayer structures. Nuclear Instruments & Methods in Physics Research B, 2002, 188, 90-95.	0.6	14
673	Study of calcium implanted GaN. Nuclear Instruments & Methods in Physics Research B, 2002, 190, 625-629.	0.6	5
674	Strain relaxation and compositional analysis of InGaN/GaN layers by Rutherford backscattering. Nuclear Instruments & Methods in Physics Research B, 2002, 190, 560-564.	0.6	10
675	Analysis of sapphire implanted with different elements using artificial neural networks. Nuclear Instruments & Methods in Physics Research B, 2002, 190, 241-246.	0.6	6
676	Surface quality studies of high-Tc superconductors of the Hg-, Tl- and HgxTl1â^'x-families: RBS and resonant C and O backscattering studies. Nuclear Instruments & Methods in Physics Research B, 2002, 190, 673-678.	0.6	1
677	Physical and morphological characterization of reactively magnetron sputtered TiN films. Thin Solid Films, 2002, 420-421, 421-428.	0.8	21
678	Nanoindentation on MgO crystals implanted with lithium ions. Nuclear Instruments & Methods in Physics Research B, 2002, 191, 154-157.	0.6	5
679	Conductivity behaviour of Cr implanted TiO2. Nuclear Instruments & Methods in Physics Research B, 2002, 191, 158-162.	0.6	23
680	Electrical conductivity of MgO crystals implanted with lithium ions. Nuclear Instruments & Methods in Physics Research B, 2002, 191, 191-195.	0.6	22
681	Effects of ion implantation on the thermoluminescent properties of natural colourless topaz. Nuclear Instruments & Methods in Physics Research B, 2002, 191, 196-201.	0.6	7
682	Structural and optical characterization of topaz implanted with Fe and Co. Nuclear Instruments & Methods in Physics Research B, 2002, 191, 312-316.	0.6	11
683	Erbium implantation in strontium titanate. Nuclear Instruments & Methods in Physics Research B, 2002, 191, 317-322.	0.6	5
684	Lattice location and annealing behavior of Mn implanted GaN. Nuclear Instruments & Methods in Physics Research B, 2002, 191, 544-548.	0.6	20

#	Article	IF	CITATIONS
685	The structure of sapphire implanted with nitrogen at room temperature and 1000 °C. Nuclear Instruments & Methods in Physics Research B, 2002, 191, 629-632.	0.6	6
686	Luminescence and structural studies of iron implanted α-Al2O3. Nuclear Instruments & Methods in Physics Research B, 2002, 191, 638-643.	0.6	25
687	Influence of annealing atmosphere on the behavior of titanium implanted sapphire. Nuclear Instruments & Methods in Physics Research B, 2002, 191, 644-648.	0.6	7
688	Splitting of X-ray diffraction and photoluminescence peaks in InGaN/GaN layers. Materials Science and Engineering B: Solid-State Materials for Advanced Technology, 2002, 93, 163-167.	1.7	20
689	Effects of ion bombardment on properties of d.c. sputtered superhard (Ti, Si, Al)N nanocomposite coatings. Surface and Coatings Technology, 2002, 151-152, 515-520.	2.2	81
690	Optical changes induced by high fluence implantation of Co ions on sapphire. Surface and Coatings Technology, 2002, 158-159, 54-58.	2.2	5
691	Elemental characterisation of beryllium and electrical behaviour of their pebbles beds. Journal of Nuclear Materials, 2002, 307-311, 643-646.	1.3	4
692	Interpretation of double x-ray diffraction peaks from InGaN layers. Applied Physics Letters, 2001, 79, 1432-1434.	1.5	55
693	Microstructure and mechanical properties of nanocomposite (Ti,Si,Al)N coatings. Thin Solid Films, 2001, 398-399, 391-396.	0.8	131
694	Heavy ion implantation in GaN epilayers. Radiation Effects and Defects in Solids, 2001, 156, 267-272.	0.4	1
695	Elastic properties of (Ti,Al,Si)N nanocomposite films. Surface and Coatings Technology, 2001, 142-144, 110-116.	2.2	45
696	Photoluminescence and lattice location of Eu and Pr implanted GaN samples. Physica B: Condensed Matter, 2001, 308-310, 22-25.	1.3	91
697	Green and red emission in Ca implanted GaN samples. Physica B: Condensed Matter, 2001, 308-310, 42-46.	1.3	5
698	Spectroscopic ellipsometry study of the layer structure and impurity content in Er-doped nanocrystalline silicon thin films. Physica B: Condensed Matter, 2001, 308-310, 374-377.	1.3	4
699	Photoluminescence studies in ZnO samples. Physica B: Condensed Matter, 2001, 308-310, 985-988.	1.3	84
700	High temperature annealing of Er implanted GaN. Materials Science and Engineering B: Solid-State Materials for Advanced Technology, 2001, 81, 132-135.	1.7	13
701	Indium Distribution within InxGa1?xN Epitaxial Layers: A Combined Resonant Raman Scattering and Rutherford Backscattering Study. Physica Status Solidi (B): Basic Research, 2001, 228, 173-177.	0.7	2
702	Depth Resolved Studies of Indium Content and Strain in InGaN Layers. Physica Status Solidi (B): Basic Research, 2001, 228, 59-64.	0.7	7

#	Article	IF	CITATIONS
703	Indium content determination related with structural and optical properties of InGaN layers. Journal of Crystal Growth, 2001, 230, 448-453.	0.7	8
704	Hyperfine Fields of 181Ta in UFe4Al8. Hyperfine Interactions, 2001, 136/137, 333-337.	0.2	4
705	Amorphization of GaN by ion implantation. Nuclear Instruments & Methods in Physics Research B, 2001, 178, 200-203.	0.6	15
706	Coherent amorphization of Ge/Si multilayers with ion beams. Nuclear Instruments & Methods in Physics Research B, 2001, 178, 279-282.	0.6	2
707	Artificial neural network analysis of RBS data of Er-implanted sapphire. Nuclear Instruments & Methods in Physics Research B, 2001, 175-177, 108-112.	0.6	5
708	Study of new surface structures created on sapphire by Co ion implantation. Nuclear Instruments & Methods in Physics Research B, 2001, 175-177, 500-504.	0.6	7
709	Study of Fe+ implanted GaN. Nuclear Instruments & Methods in Physics Research B, 2001, 175-177, 241-245.	0.6	9
710	Study of solid-state reactions of SiC/SiCf composites using microbeams. Nuclear Instruments & Methods in Physics Research B, 2001, 181, 377-381.	0.6	1
711	Cadmium addition to vacancy doped lanthanum manganites: from metallic to insulator behaviour. Journal of Magnetism and Magnetic Materials, 2001, 226-230, 797-799.	1.0	5
712	OPTICAL DOPING OF NITRIDES BY ION IMPLANTATION. Modern Physics Letters B, 2001, 15, 1281-1287.	1.0	33
713	Fe ion implantation in GaN: Damage, annealing, and lattice site location. Journal of Applied Physics, 2001, 90, 81-86.	1.1	24
714	Green, red and infrared Er-related emission in implanted GaN:Er and GaN:Er,O samples. Journal of Applied Physics, 2001, 89, 6183-6188.	1.1	34
715	Compositional pulling effects inInxGa1â^'xN/GaNlayers: A combined depth-resolved cathodoluminescence and Rutherford backscattering/channeling study. Physical Review B, 2001, 64, .	1.1	176
716	Compositional dependence of the strain-free optical band gap in InxGa1â^'xN layers. Applied Physics Letters, 2001, 78, 2137-2139.	1.5	104
717	Influence of Temperature and Pressure on the Beryllium Pebbles Bed Electrical Resistivity. Fusion Science and Technology, 2000, 38, 320-325.	0.6	6
718	Strain and Compositional Analysis of InGaN/GaN Layers. Materials Research Society Symposia Proceedings, 2000, 639, 3521.	0.1	3
719	Raman spectroscopy studies in InGaN/GaN wurtzite epitaxial films. Materials Research Society Symposia Proceedings, 2000, 639, 6101.	0.1	2
720	Optical Characterization of AlGaN/GaN MQW's. Materials Research Society Symposia Proceedings, 2000, 639, 6211.	0.1	0

#	Article	IF	CITATIONS
721	Surface studies of SiC/SiCf composites exposed to relevant fusion reactor conditions. Surface and Interface Analysis, 2000, 30, 98-100.	0.8	6
722	Luminescence studies in colour centres produced in natural topaz. Journal of Luminescence, 2000, 87-89, 583-585.	1.5	6
723	Structure determination of (Ti,Al)N/Mo multilayers. Thin Solid Films, 2000, 373, 287-292.	0.8	3
724	Characterisation of Ti1â^'xSixNy nanocomposite films. Surface and Coatings Technology, 2000, 133-134, 307-313.	2.2	190
725	Structural and magnetic studies of Fe-implanted α-Al2O3. Surface and Coatings Technology, 2000, 128-129, 434-439.	2.2	23
726	Hard nanocomposite Ti–Si–N coatings prepared by DC reactive magnetron sputtering. Surface and Coatings Technology, 2000, 133-134, 234-239.	2.2	115
727	Anisotropic transport properties of epitaxial La2/3Ca1/3MnO3 thin films with different growth orientations (invited). Journal of Magnetism and Magnetic Materials, 2000, 211, 1-8.	1.0	11
728	Effect of crystal orientation on defect production and optical activation of Er-implanted sapphire. Nuclear Instruments & Methods in Physics Research B, 2000, 166-167, 183-187.	0.6	14
729	Annealing behaviour of natural topaz implanted with W and Cr ions. Nuclear Instruments & Methods in Physics Research B, 2000, 166-167, 204-208.	0.6	8
730	Influence of oxygen ion implantation on the damage and annealing kinetics of iron-implanted sapphire. Nuclear Instruments & Methods in Physics Research B, 2000, 166-167, 188-192.	0.6	7
731	RBS/Channeling study of Er doped GaN films grown by MBE on Si substrates. Nuclear Instruments & Methods in Physics Research B, 2000, 161-163, 946-951.	0.6	22
732	Micron-scale analysis of SiC/SiCf composites using the new Lisbon nuclear microprobe. Nuclear Instruments & Methods in Physics Research B, 2000, 161-163, 334-338.	0.6	65
733	Molecular H2 and H3 energy loss measurements along the Si ã€^111〉 direction. Nuclear Instruments & Methods in Physics Research B, 2000, 161-163, 168-171.	0.6	5
734	A structural and mechanical analysis on PVD-grown (Ti,Al)N/Mo multilayers. Thin Solid Films, 2000, 377-378, 425-429.	0.8	20
735	Anisotropic electrical transport in epitaxial La2/3Ca1/3MnO3 thin films. Journal of Applied Physics, 2000, 87, 5570-5572.	1.1	22
736	Annealing behavior and lattice site location of Hf implanted GaN. Materials Science and Engineering B: Solid-State Materials for Advanced Technology, 1999, 59, 207-210.	1.7	22
737	Characterisation of YBaCuO-PrBaCuO Multilayers Grown by Pulsed Injection MO-CVD. Journal of Low Temperature Physics, 1999, 117, 657-661.	0.6	0
738	Stability studies of Hg implanted YBa2Cu3O6+x. Nuclear Instruments & Methods in Physics Research B, 1999, 147, 244-248.	0.6	3

#	Article	IF	CITATIONS
739	Lattice location and annealing behaviour of Pt and W implanted sapphire. Nuclear Instruments & Methods in Physics Research B, 1999, 147, 226-230.	0.6	4
740	Ion beam and photoluminescence studies of Er and O implanted GaN. Nuclear Instruments & Methods in Physics Research B, 1999, 147, 383-387.	0.6	26
741	Formation of coherent precipitates of platinum in sapphire. Nuclear Instruments & Methods in Physics Research B, 1999, 148, 1049-1053.	0.6	14
742	Stability and diffusion of Hg implanted YBa2Cu3O6+x. Nuclear Instruments & Methods in Physics Research B, 1999, 148, 807-812.	0.6	3
743	Effect of crystal orientation on damage accumulation and post-implantation annealing for iron implantation into sapphire. Nuclear Instruments & Methods in Physics Research B, 1999, 148, 730-734.	0.6	10
744	Nuclear microbeam study of advanced materials for fusion reactor technology. Nuclear Instruments & Methods in Physics Research B, 1999, 158, 671-677.	0.6	2
745	Properties of epitaxial LaCaMnO laser ablated thin films on (1 0 0) and (1 1 0) SrTiO3 substrates. Journal of Magnetism and Magnetic Materials, 1999, 196-197, 495-497.	1.0	6
746	Ion beam studies of CdTe films epitaxially grown on Si, GaAs and sapphire substrates. Nuclear Instruments & Methods in Physics Research B, 1998, 136-138, 220-224.	0.6	6
747	Lattice site location of thulium and erbium implanted GaAs. Nuclear Instruments & Methods in Physics Research B, 1998, 136-138, 421-425.	0.6	5
748	Lattice site location and annealing behavior of W implanted TiO2. Nuclear Instruments & Methods in Physics Research B, 1998, 136-138, 442-446.	0.6	8
749	Solubility and damage annealing of Er implanted single crystalline α-Al2O3. Nuclear Instruments & Methods in Physics Research B, 1998, 139, 313-317.	0.6	9
750	Chemical effects on the amorphization of sapphire. Nuclear Instruments & Methods in Physics Research B, 1998, 141, 353-357.	0.6	10
751	Microscopic studies of radioactive Hg implanted in YBa 2Cu3O6 + x superconducting thin films. Journal of Magnetism and Magnetic Materials, 1998, 177-181, 511-512.	1.0	4
752	Radioactive Isotope Identifications of Au and Pt Photoluminescence Centres in Silicon. Physica Status Solidi (B): Basic Research, 1998, 210, 853-858.	0.7	9
753	RBS Lattice Site Location and Damage Recovery Studies In GaN. Materials Research Society Symposia Proceedings, 1998, 537, 1.	0.1	0
754	Substrate effect on CdTe layers grown by metalorganic vapor phase epitaxy. Applied Physics Letters, 1997, 70, 1314-1316.	1.5	30
755	The Photoluminescence of Pt-Implanted Silicon. Materials Science Forum, 1997, 258-263, 473-478.	0.3	5
756	Lattice site and photoluminescence of erbium implanted in α–Al <sub>2</sub> O <sub>3</sub> . Journal of Materials Research, 1997, 12, 1401-1404.	1.2	26

#	Article	IF	CITATIONS
757	Improving the Thermal Stability of Photoresist Films by Ion Beam Irradiation. Materials Research Society Symposia Proceedings, 1997, 504, 443.	0.1	1
758	Etching of amorphous Al2O3 produced by ion implantation. Nuclear Instruments & Methods in Physics Research B, 1997, 127-128, 596-598.	0.6	21
759	Microscopic studies of implanted 73As in diamond. Nuclear Instruments & Methods in Physics Research B, 1997, 127-128, 723-726.	0.6	20
760	Selective area vapor-phase epitaxy and structural properties of Hg1 â^' xCdxTe on sapphire. Journal of Crystal Growth, 1997, 179, 585-591.	0.7	7
761	Rutherford Backscattering and Photoluminescence Studies of Erbium Implanted GaAs. Materials Research Society Symposia Proceedings, 1996, 422, 173.	0.1	Ο
762	Radiation damage annealing of Hg implanted InP. Nuclear Instruments & Methods in Physics Research B, 1996, 120, 244-247.	0.6	1
763	Low temperature epitaxial regrowth of mercury implanted sapphire. Nuclear Instruments & Methods in Physics Research B, 1996, 120, 248-251.	0.6	2
764	Ion beam mixing of chromium or zirconium films with sapphire. Surface and Coatings Technology, 1996, 83, 151-155.	2.2	5
765	Structural properties of CdTe and Hg1 â^' xCdxTe epitaxial layers grown on sapphire substrates. Journal of Crystal Growth, 1996, 161, 195-200.	0.7	11
766	Laser-assisted recrystallization to improve the surface morphology of CdTe epitaxial layers. Semiconductor Science and Technology, 1996, 11, 248-251.	1.0	11
767	Structural properties of layers grown on CdTe substrates by liquid phase epitaxy. Semiconductor Science and Technology, 1996, 11, 542-547.	1.0	6
768	Incorporation and stability of erbium in sapphire by ion implantation. , 1996, , 429-432.		0
769	Incorporation and stability of erbium in sapphire by ion implantation. Nuclear Instruments & Methods in Physics Research B, 1995, 106, 429-432.	0.6	28
770	The substitutionality of hafnium in sapphire by ion implantation and low temperature annealing. Nuclear Instruments & Methods in Physics Research B, 1995, 106, 602-605.	0.6	4
771	Hyperfine fields of mercury in singleâ€crystalline cobalt. Journal of Applied Physics, 1994, 76, 6906-6908.	1.1	5
772	The lattice site of Au in Be after 24 h 197mHg isotope implantation and decay. Nuclear Instruments & Methods in Physics Research B, 1994, 85, 457-461.	0.6	1
773	Lattice location of Er in GaAs and Al0.5Ga0.5As layers grown by MBE on (100) GaAs substrates. Nuclear Instruments & Methods in Physics Research B, 1993, 80-81, 180-183.	0.6	10
774	Lattice Location and Photoluminescence of Er in GaAs and Al0.5Ga0.5As. Materials Research Society Symposia Proceedings, 1993, 301, 175.	0.1	4

#	Article	IF	CITATIONS
775	Vacancy-acceptor complexes in germanium produced by ion implantation. Nuclear Instruments & Methods in Physics Research B, 1991, 59-60, 1049-1052.	0.6	6
776	Lattice site location and outdiffusion of mercury implanted in GaAs. Nuclear Instruments & Methods in Physics Research B, 1991, 59-60, 1090-1093.	0.6	3
777	Epitaxial regrowth and lattice location of indium implanted in arsenic-preamorphized silicon. Nuclear Instruments & Methods in Physics Research B, 1991, 55, 580-584.	0.6	5
778	Regrowth of indium-implanted (100), (110) and (111) silicon crystals studied with Rutherford backscattering and perturbed angular correlation techniques. Materials Science and Engineering B: Solid-State Materials for Advanced Technology, 1989, 4, 189-195.	1.7	2
779	Lattice Location Studies on Hafnium, Thallium and Lead Implanted Magnesium Single Crystals. , 1984, , 74-82.		6
780	Electrical conductivity in ion implanted TiO/sub 2/-single crystals. , 0, , .		1
781	Structural and Mechanical Properties of AZOY Thin Films Deposited on Flexible Substrates. Materials Science Forum, 0, 587-588, 834-838.	0.3	0
782	Study of SiGe Alloys with Different Germanium Concentrations Implanted with Mn and As Ions. Materials Science Forum, 0, 587-588, 298-302.	0.3	0
783	Room Temperature Magnetic Response of Sputter Deposited TbDyFe Films as a Function of the Deposition Parameters. Journal of Nano Research, 0, 18-19, 235-239.	0.8	3
784	Wettability and Nanotribological Response of Silicon Surfaces Functionalized by Ion Implantation. Materials Science Forum, 0, 730-732, 257-262.	0.3	1
785	Surface Plasmon Resonance Effect on the Optical Properties of TiO <sub>2</sub> Doped by Noble Metals Nanoparticles. Journal of Nano Research, 0, 18-19, 177-185.	0.8	8